DYNAMIC RESPONSE OF CANTILEVER BRIDGES TO MOVING FORCES

Thesis for the Degree of M. S.

MICHIGAN STATE UNIVERSITY

Teoktistos Toridis

1961

This is to certify that the

thesis entitled

DYNAMIC RESPONSE OF CANTILEVER BRIDGES
TO MOVING FORCES

presented by

Teoktistos Toridis

has been accepted towards fulfillment
of the requirements for

M. S. degree in Civil Engineering

R. K. Wen

Major professor

Date June 30, 1961

O-169

ABSTRACT

DYNAMIC RESPONSE OF CANTILEVER BRIDGES TO MOVING FORCES

by Teoktistos Toridis

An analytical study is made of the dynamic behavior of three-span (symmetrical) cantilever bridges under moving forces. In the study, the bridge is represented by a beam with uniform flexural rigidity, and the mass of the beam is lumped at five locations.

The variables considered are the speed of the moving force, the stiffness and weight of the bridge, and the relative lengths of the various spans of the structure.

A mathematical analysis based on the method of "modal analysis" is programmed for numerical solutions of problems on the MISTIC, the digital computer of Michigan State University. The numerical data obtained for the study cover nearly all bridges having practical proportions. Among the results presented is a set of graphs by use of which the first five natural periods of vibration of this type of bridges can be easily obtained.

It is found that the dynamic effects can be as much as 56% greater than the maximum static effects. In general, the dynamic response tends to increase with an increase in the speed of the moving force. For a given speed, the amount of excitation to which the bridge is subjected increases with the duration of the travel of the moving load on the bridge.

Results also indicate that the response of the structure is composed of mainly the first, second, and to a lesser degree, the third normal modes of vibration.

DYNAMIC RESPONSE OF CANTILEVER BRIDGES TO MOVING FORCES

By

TEOKTISTOS TORIDIS

A THESIS

Submitted to
Michigan State University
in partial fulfillment of the requirements
for the degree of

MASTER OF SCIENCE

Department of Civil Engineering

1961

ACKNOWLEDGMENTS

The work reported in this thesis was carried out as part of a research project sponsored by the Division of Engineering Research to study the dynamic behavior of cantilever bridges.

The investigation was under the immediate supervision of Dr. R. K. Wen, the author's advisor, to whom gratitude is extended for his valuable guidance during all phases of the work.

TABLE OF CONTENTS

Page

LIST OF TABLES

LIST OF FIGURES

I. INTRODUCTION

1.1 General

The behavior of highway bridges under moving traffic is a complicated dynamic phenomenon. It depends on a large number of variables such as the type and weight of the structure and the vehicle, the speed of the vehicle, the unevenness of the approach roadway and of the bridge deck itself, and the damping characteristics of the bridge and vehicle. Because of a lack of sufficient knowledge on the relative importance of these variables, provisions for the dynamic effects in the design of highway bridges have been based on entirely empirical rules. For example, the "Impact Formula" given in the "Standard Specifications for Highway Bridges" by the American Association of State Highway Officials implies that the dynamic effects depend on only one variable, namely, the length of the bridge.

There have been a great deal of research activities in recent years in the study of the dynamic behavior of highway bridges. The goals appear to be to assess the relative importance of the different variables that enter into the problem and, ultimately, to develop a more rational procedure for making provisions concerning the dynamic effects in bridges.

In the past, researches on the subject have been largely focused on simple span and continuous bridges. But it was noted in a recent series of field tests (3) that it was the cantilever bridges that were most susceptible to vibrations. Since 1959, an investigation into the dynamic

behavior of this type of bridges has been conducted at Michigan State University. This thesis represents a phase of the investigation.

1.2 Object and Scope

The purpose of this investigation has been to study analytically the dynamic response of three-span symmetrical cantilever bridges to moving loads.

The variables considered in the study are the speed of the moving load, stiffness and weight of the bridge, and the relative span lengths of the various spans in a cantilever bridge.

In the analysis, the bridge is represented by a beam. The mass of the beam is lumped at a finite number of points. However, the structure is considered to possess uniform flexibility along its length. The moving load is idealized as a moving constant force.

The mathematical analysis used has been based on a method described in Reference (1). The method deals with the dynamic analysis of elastic beams and frames by the "modal analysis" approach. It can be applied to cases in which the point of action of the exciting force does not necessarily coincide with one of the lumped mass points.

The present investigation includes the following three phases:

1. The application of the mathematical theory in Ref. (1) to develop a computer program for use on the MISTIC (the digital computer of Michigan State University).
2. The use of the program developed to obtain numerical results covering certain appropriate ranges of the variables of the problem.

3. The study of the numerical results obtained with the purpose of understanding better the dynamic behavior of this type of bridges and determining the effects and importance of the variables of the problem.

1.3 Past Work

A mathematical analysis of the dynamic behavior of cantilever bridges was reported in Ref. (6), but no numerical results were given for the moving load problem. Some numerical results concerning the dynamic response of cantilever bridges to moving loads were reported in Ref. (4). However, they were limited to one fixed set of relative span lengths of the bridge. In the present study, as already mentioned, these span lengths have been treated as variables.

1.4 Notation

The symbols used in this report are defined in the text where they first appear.

II. MATHEMATICAL ANALYSIS

The mathematical analysis of the problem presented in this chapter is essentially the same as that given in Ref. (1). It is included here for the sake of completeness.

2. 1. System Considered and Assumptions

The physical system is shown in Fig. 1a. It consists of an elastic system of beams with two side or anchor spans, two cantilever arms, and a suspended span. The suspended span is connected to the two cantilever arms by means of frictionless hinges. The mass of the beam is concentrated at five points in the manner shown in Fig. 1b. However, the flexibility of the beam is considered to be uniformly distributed.

In the analysis, the usual beam theory is assumed: that is, the bending moment is proportional to the second derivative of the deflection curve, and deformations due to shearing stresses are negligible.

As mentioned previously, the moving load is represented by a constant force, traveling from the left to the right. No damping has been considered in the system.

2. 2 Equations of Motion

Consider the beam and mass system shown in Fig. 1b. Applying d'Alembert's principle, the deflection of some point mass m_i may be expressed as:

$$y_i = - \left[\sum_{j=1}^{n} m_j \ddot{y}_j d_{ij} \right] + p g_{iz} \qquad (1)$$

in which

y_i = deflection of m_i measured from the static equilibrium position of the beam under the action of its own weight

$\ddot{y}_j$ = second derivative of the deflection of m_j with respect to time

d_{ij} = influence coefficient for deflection at m_i due to a unit load at m_j

p = weight of moving load

g_{iz} = influence coefficient for deflection at m_i due to a unit load at a distance z from the left-most support, specifying the instantaneous position of the moving load

n = number of point masses (five in the present case)

The first part on the right hand side of Eq. (1) shows the effect of the inertia forces on the deflection of m_i, while the second one represents the effect of the moving load.

An equation of the form of Eq. (1) can be written for each concentrated mass, m_i. The number of equations, n, obtained in this manner is equal to the number of concentrated masses, or degrees of freedom of the system. These equations may be expressed in the following matrix form:

$$Y = -DM\ddot{Y} + pG \tag{2}$$

where

$$Y = \begin{bmatrix} y_1 \\ y_2 \\ \\ y_n \end{bmatrix} = \text{deflection matrix}$$

$$D = \begin{bmatrix} d_{11} & d_{12} & \cdots & d_{1n} \\ d_{21} & d_{22} & & d_{2n} \\ & & & \\ d_{n1} & d_{n2} & & d_{nn} \end{bmatrix} = \text{flexibility matrix}$$

$$M = \begin{bmatrix} m_1 & 0 & \cdots & 0 \\ 0 & m_2 & & 0 \\ & & & \\ 0 & 0 & & m_n \end{bmatrix} = \text{mass matrix}$$

$$\ddot{Y} = \begin{bmatrix} \ddot{y}_1 \\ \ddot{y}_2 \\ \\ \ddot{y}_n \end{bmatrix} = \text{acceleration matrix}$$

$$G = \begin{bmatrix} g_{1z} \\ g_{2z} \\ \\ g_{nz} \end{bmatrix} = \text{flexibility matrix for the moving load}$$

2. 3. Free Vibrations

The expression for free vibrations of the structure can be obtained by considering the forcing function in Eq. (2) to be equal to zero. Eq. (2) then reduces to the following form:

$$Y = -DM\ddot{Y} \tag{3}$$

The solution of the above second order differential equation is accomplished by letting:

$$Y = W \sin\sqrt{\lambda}\, t \tag{4}$$

in which

$$W = \begin{bmatrix} w_1 \\ w_2 \\ \\ \\ w_n \end{bmatrix}$$ = a particular deflection configuration of the structure (= normal mode)

λ = a constant to be determined (= natural angular frequency squared)

t = time (independent variable)

Substituting Eq. (4) into Eq. (3), premultiplying both sides by M, and simplifying, one obtains the equation:

$$MW = \lambda KW \tag{5}$$

in which $K = MDM$. It may be noted that both M and K are symmetric matrices. A solution of Eq. (5) yields the natural frequencies and normal modes of vibration of the system.

2.4. Forced Vibrations

Premultiplying both sides of Eq. (2) by M one obtains:

$$MY = - K\ddot{Y} + pMG \tag{6}$$

To solve this equation the "modal analysis" method is used by letting:

$$Y = U\Phi \tag{7}$$

where

$$U = [W^1 W^2 \ldots W^n]$$

$$\Phi = \begin{bmatrix} \phi^1 \\ \phi^2 \\ \\ \\ \phi^n \end{bmatrix}$$

The elements of the Φ matrix are time-dependent, while those of U are not consequently:

$$\ddot{Y} = U\ddot{\Phi} \tag{8}$$

Substituting Eq. (7) and (8) into Eq. (6), one obtains the expression:

$$MU\Phi = -KU\ddot{\Phi} + pMG \tag{9}$$

Using the orthogonality relationships of the normal modes and performing some manipulations which can be followed in Ref. 1, Eq. (9) is separated into a set of second order differential equations of the type:

$$\phi^j + \lambda^j \phi^j = \frac{(W^j)' MG}{(W^j)' KW^j} p \tag{10}$$

where $(W^j)'$ = transpose of W^j. In this equation both the numerator and the denominator on the right hand side are scalars. It is therefore a scalar equation involving only one dependent variable, ϕ^j. The right hand side of Eq. (10) becomes a constant for any given location of the moving load, and thus its solution is possible.

2.5. Dimensionless Form of Differential Equations

Eq. (5) may be put into the form:

$$(M - \lambda K) W = 0$$

The dimensionless version of this equation is:

$$(M_s - \lambda_s K_s) W = 0 \tag{11}$$

in which

$$M_s = \frac{1}{100\, m_1} M$$

$$K_s = \frac{48\, E\, I}{m_1^2 L^3} K$$

$$\lambda_s = \frac{m_1 L^3}{4800\, E\, I} \lambda$$

The subscript "s" in this case stands for "scaled" quantities, and m_1 is defined in Fig. 1b.

Since Eq. (10) has the dimension of acceleration it is rendered dimensionless by dividing through by the gravitational acceleration, g. The notation and the scaling factors used throughout the operations below are the same as in Ref. 1.

First, the independent variable t in Eq. (10) is transformed into a dimensionless form by letting:

$$\tau = \frac{v}{2L}\, t$$

$$d\tau = \frac{v}{2L}\, dt$$

Substituting into Eq. (10):

$$\left(\frac{v}{2L}\right)^2 \frac{d^2\phi^j}{d\tau^2} + \lambda^j \phi^j = \frac{(W^j)' MG}{(W^j)' KW^j}\, p$$

Next, the dependent variable ϕ is rendered dimensionless, letting:

$$\bar{\phi}^j = \frac{1}{\Delta_o}\, \phi^j \; ; \qquad \Delta_o = \frac{(m_b Lg)\, L^3}{48\, E\, I}$$

where m_b is the mass per unit length of the beam.

With these substitutions and the division by g, one obtains:

$$\frac{\Delta_o}{g}\left(\frac{v}{2L}\right)^2 \frac{d^2\bar{\phi}^j}{d\tau^2} + \frac{\Delta_o}{g}\, \lambda^j \bar{\phi}^j = \frac{(W^j)' MG}{(W^j)' KW^j}\, \frac{p}{g}$$

Introducing a new parameter "a," the above equation becomes:

$$a^2 \frac{d^2\bar{\phi}^j}{d\tau^2} + \bar{\lambda}^j \bar{\phi}^j = \frac{(W^j)' MG}{(W^j)' KW^j}\, \frac{p}{g} \qquad (12)$$

where

$$a = \frac{v}{2L}\sqrt{\frac{\Delta_o}{g}} = \frac{v}{2L}\sqrt{\frac{m_b L^4}{48\, E\, I}}$$

$$\bar{\lambda}^j = \frac{\Delta_o}{g}\, \lambda^j$$

Finally, the right hand side of Eq. (12) is made dimensionless, using:

$$\bar{M} = \frac{1}{m_b L} M$$

$$\bar{G} = \frac{48 E I}{L^3} G$$

$$\bar{K} = \bar{M}\bar{D}\bar{M}$$

$$\bar{D} = \frac{48 E I}{L^3} D$$

$$\bar{p} = \frac{1}{m_b L g} p$$

from which the following equation results:

$$\alpha \frac{d^2 \bar{\phi}^j}{d\tau^2} + \bar{\lambda}^j \bar{\phi}^j = \frac{(W^j)' \bar{M} \bar{G}}{(W^j)' K W^j} \bar{p} \qquad (13)$$

2.6. Parameters of Problem

It may be noted that in order to solve Eq. (13) the following quantities have to be given or determined: α, $\bar{\lambda}^j$, W^j, $\bar{M}$, $\bar{G}$, $\bar{K}$. However, once the parameters $\frac{l_1}{l_2}$, $\frac{a}{l_2}$ and α are specified all the remaining coefficients and constants in the above equation can be computed by using the values of these parameters. The range of the parameters and a brief description of their significance are given below:

2.6.1. Span Lengths

To determine the range of the span lengths, a study of seven three-span cantilever bridges given in Ref. (3) was made. In order to include

nearly all bridges of practical proportions, the following range was finally selected:

$$\frac{l_1}{l_2} = 0.50 \text{ to } 2.00$$

$$\frac{a}{l_2} = 0.10 \text{ to } 0.40$$

2.6.2. Speed Parameter α

Although this parameter incorporates in it the effect of the stiffness of the bridge, for a given bridge with a uniform EI the only variable in the expression for α is the speed of the moving force.

For a given speed, the value of α does not remain the same within the range of the span lengths considered. To establish the limiting values of this parameter, the characteristics of the previously mentioned seven cantilever bridge have been used. It has been found that the speed range of 15 to 75 mph in an actual bridge-vehicle system corresponds approximately to the range of values of α from 0.0225 to 0.1125.

In passing, it may be pointed out that the magnitude of the moving force is not a parameter. Variations in the magnitude of the force produce linearly proportional effects in the response of the beam. Therefore, in obtaining all numerical results a value of $\bar{p} = 0.3150$ has been used. This value of $\bar{p}$ corresponds to approximately 20 tons in a representative actual bridge-vehicle system.

III. COMPUTER PROGRAM

3.1. Outline of Program

The analysis of the problem is programmed for numerical solutions on the MISTIC. The sequence of the basic operations in the program is outlined as follows.

1. The computer is fed the data for the problem, specifying the characteristics of the bridge and load, and the time interval for use in the numerical integration process.

2. The matrices M_s, D, and K_s (see Eq. 11) are formed.

3. The natural frequencies and normal modes of vibration of the bridge are calculated and printed out as part of the output of the computer.

4. The constant coefficients in Eq. (13)--the governing differential equation--are formed.

5. For the particular time (or location of the load on the bridge under consideration) the coefficient involving $\bar{G}$ is formed. The elements of matrix $\bar{G}$ represent the static deflections at the various mass points for that particular location of the load.

6. The differential equations are integrated numerically for a pre-set time increment.

7. The dynamic deflections are obtained by use of Eq. (7).

8. Steps (5) through (7) are repeated for the complete passage of the load over the bridge.

9a. As output of the program, after each increment of time in the numerical integration process, the computer prints out the dynamic deflection and the corresponding static deflection for each of the five mass-points.

9b. A modified version of the program will print out only the following data for every mass-point: The maximum dynamic deflection and the location of the load (τ) producing this maximum; the maximum static deflection and the location of the load producing this maximum; the "maximum amplification factor with respect to τ," defined to be the ratio of the maximum dynamic deflection to the maximum static deflection.

It takes the computer approximately one hour to compute and print out the dynamic and static deflections for every step of integration (the total number of steps covering the crossing of the bridge is equal to 1000). If only the maximum responses are printed out, the corresponding computer time is reduced to about 8 minutes.

Some detailed information related to the programming of the problem is further presented in Art. 3.3.

3.2. Time Increment and Convergence Considerations

For the numerical integration the "Linear Acceleration" method has been used. In this method the time increment should be small enough to satisfy the criteria of stability and convergence. A smaller increment will in general give a more accurate answer, but the number of steps of integration, and hence the computation time will be increased.

In Ref. (5), the convergence criterion for this method is given as:

$$\Delta t = 0.389\ T$$

where Δt is the maximum time increment and T is the shortest natural period of vibration of the system. It is also stated that if the convergence criterion is satisfied the requirement for stability is automatically met.

In this investigation the interval of integration was chosen to meet the above requirements for nearly all bridges within the range of the parameters considered. As shown in Art. 2.5., the independent variable was put into a dimensionless form by introducing the variable τ. It was found that an increment ($\Delta\tau$) of 0.0005 gives satisfactory results in all cases where convergence can be obtained. The number of integrations corresponding to this increment is 1000. A comparison of the results obtained by using different increments is shown below:

TABLE 1. Effect of magnitude of increments

$\Delta\tau$ = increment	Number of integrations	Maximum dynamic deflections at m_3 (dimensionless)
0.0005	1000	0.011968143
$0.0006\frac{7}{}$	746	0.011967531
0.0010	500	0.011968675

It is seen that the deflections corresponding to the three different increments do not vary appreciably. However, in certain cases, for low α values, using the increments of $0.0006\frac{7}{}$ and 0.0010 has caused very slow rates of convergence, or sometimes no convergence at all. Hence

$\Delta\tau$ was chosen as 0.0005. Considering an average bridge, this increment corresponds to a time equal to $\frac{1}{10}$ of the fifth natural period of vibration.

Although the increment of 0.0005 has been satisfactory in obtaining numerical results within practically the whole range of the parameters, it did not meet the convergence criterion in the following cases: $\frac{l_1}{l_2} = 1.30$, $\frac{a}{l_2} = 0.10$, $\alpha = 0.0225 - 0.1125$; $\frac{l_1}{l_2} = 1.50$, $\frac{a}{l_2} = 0.10$, $\alpha = 0.0225 - 0.1125$; $\frac{l_1}{l_2} = 1.70$; $\frac{a}{l_2} = 0.10$, $\alpha = 0.0225$; $\frac{l_1}{l_2} = 1.90$, $\frac{a}{l_2}$ 0.10, $\alpha = 0.1125$. Using a smaller increment of 0.0001 has been satisfactory in obtaining convergence and hence numerical results in the latter two cases. Also, it has been found possible to obtain convergence in the first two cases for high values of α, using $\Delta\tau = 0.0001$ or 0.00007. But for smaller values of α it seems that even a smaller $\Delta\tau$ would be necessary. Hence, no numerical solutions have been obtained for these two cases, because they would require a great amount of computer time.

3.3. Detailed Operations in Computer Program

The basic steps of the computer program have been outlined in Art. 3.1. In this article is presented some detailed information related to the programming of the problem.

3.3.1. Natural Frequencies and Normal Modes

These quantities are obtained by solving Eq. (11). For this purpose, matrices M_s and K_s have to be formed. K_s results from the multiplication of three matrices ($M_s \bar{D} M_s$) and a numerical constant used for scaling purposes (see Art. 2.5.).

The elements of matrix $\bar{D}$ are computed by using a "deflection" subroutine. This subroutine has been prepared for calculating the deflections at the five mass points shown in Fig. 1b due to a vertical unit load applied at any point on the beam.

Having formed M_s and K_s, the natural frequencies and modes of vibration of the structure are obtained by use of a library routine (M5 - 139). This routine has been modified so that it would use the matrices already stored in the computer as its data for computation. In this manner, a data tape that would normally be required was eliminated.

The characteristic values (λ_s^j) given by the computer represent the natural angular frequencies of vibration (λ^j) scaled by the factor shown in Art. 2.5. The relationship between λ^j and $\bar{\lambda}^j$ [$\bar{\lambda}^j$ appears in Eq. (13)] has been given in Art. 2.5. For coding purposes, the actual value of the natural frequency (λ^j) has not been needed. Since λ_s^j is stored in the memory of the computer, $\bar{\lambda}^j$ can be formed using the following equation:

$$\bar{\lambda}^j = \frac{200\,L}{l_1}\ \lambda_s^j$$

where

L = overall length of beam

l_1 = length of side span

The normal modes as printed out by the computer are scaled in the manner indicated below:

$$\bar{W}^j = \frac{W^j}{\left[\sum_{i=1}^{5} (w_i^j)^2\right]^{1/2}} \tag{14}$$

where

$\bar{W}^j$ = normal modes printed out by the computer

W^j = normal modes of vibration of the beam

Substituting the above expression for W^j into Eq. (13) and cancelling out the scaling factors one obtains:

$$\alpha^2 \frac{d^2\bar{\phi}^j}{d\tau^2} + \bar{\lambda}^j \bar{\phi}^j = \frac{(\bar{W}^j)' \bar{M} \bar{G}}{(\bar{W}^j)' \bar{K} \bar{W}^j} \bar{p} \tag{15}$$

Eq. (15) represents the final form of the differential equations solved in the computer program.

3.3.2. Coefficients of Eq. (15)

The value of the speed parameter α is a constant (for a given speed) as is $\bar{\lambda}^j$, since $\bar{\lambda}^j$ is a characteristic property of the bridge under consideration. Also, the right hand side of Eq. (15) is a constant for a specified location of the load. This makes the solution of the equation possible by numerical integration. To form the denominator on the right hand side of Eq. (15) matrix $\bar{K}$ has to be calculated. This results from the matrix multiplication $\bar{M}\bar{D}\bar{M}$. The denominator is a scalar, and its value is fixed for a given beam.

The numerator on the right hand side of Eq. (15) is also a scalar. It has to be computed for each step of integration, because the column matrix $\bar{G}$ is a function of the position of the load. $\bar{G}$ is calculated by the

same "deflection" subroutine that forms $\bar{D}$.

3.3.3. Integration of Eq. (15)

The integration of Eq. (15) has been carried out by use of Library routine F-3. The time required for the moving load to cross the beam has been divided into a number of intervals. The instant at which the load is exactly over the left-most support of the beam is referred to as "zero time." At that instant the initial conditions (displacement, velocity, and acceleration) of all the mass-points have to be specified. The computer program can handle initial conditions other than zero.

3.3.4. Dynamic Deflections and A. F.

Considering a single mass, Eq. (7) may be written as:

$$(y_i)_d = \sum_{j=1}^{n} w_i^j \phi^j \tag{16}$$

where the subscript "d" stands for "dynamic."

Upon using the dimensionless variable $\bar{\phi}^j$ (see Art. 2.5.), the following expression is obtained:

$$(y_i)_d = \Delta_o \sum_{j=1}^{n} w_i^j \bar{\phi}^j = \frac{m_b g L^4}{48 E I} \sum_{j=1}^{n} w_i^j \bar{\phi}^j \tag{17}$$

The corresponding static deflections are readily obtained using the elements of matrix $\bar{G}$. This is shown below (the subscript "st" stands for "static"):

$$(y_i)_{st} = p \frac{L^3}{48 E I} (\bar{g}_{iz}) = \frac{m_b g L^4}{48 E I} \bar{p} (\bar{g}_{iz}) \tag{18}$$

The mathematical expression of the amplification factor obtained from Eqs. (17) and (18), after cancelling out the common factors is:

$$\text{A. F.} = \frac{(y_i)_d}{(y_i)_{st}} = \frac{\sum_{j=1}^{n} w_i^j \bar{\phi}^j}{\bar{p}\,(\bar{g}_{iz})} \tag{19}$$

3.3.5. Check by Desk Calculator

The computer program has been checked by comparing numerical results obtained (for a test problem) by using the program and a desk calculator.

IV. RESULTS OF INVESTIGATION

The numerical results presented in this chapter comprise the free vibration behavior and the dynamic response of these bridges to a single force moving across the spans with a uniform speed. The behavior of the bridge has been investigated for the time interval starting from the entry of the load on the left-most span to its departure from the right-most span.

A description of the computer program used in obtaining the numerical data has been given in Chapter III.

4.1. Natural Periods and Normal Modes of Vibration

The relations between the fundamental period and the next four higher periods of vibration are shown in Figs. 2 through 5. These figures cover the following range of parameters: $\frac{l_1}{l_2}$ = 0.50 to 2.00, $\frac{a}{l_2}$ = 0.10 to 0.40. An increment of 0.10 was used for both parameters. It may be observed that the graphs in Figs. 2-5 exhibit regular patterns. Hence, they may be used, through interpolation if necessary, to obtain the ratios of the first five natural periods for bridges that fall within the above-mentioned range of parameters.

In order to obtain the first five natural periods of a bridge by use of Figs. 2-5, Fig. 6 has been prepared. This figure relates T_1, the fundamental period to a reference quantity T_s'. The latter quantity is numerically equal to the fundamental period of vibration of the suspended span treated as a simply supported beam. Therefore, with the aid of

the curves in Figs. 2-6 one needs only to compute the quantity T_s, in order to obtain the values of the first five periods of a three-span cantilever bridge.

The first five normal modes of vibration of a typical bridge are shown in Fig. 7.

4. 2. History Curves

Presented in Figs. 8-12 are the "history curves" for the five point masses that represent the lumped masses of the bridge. The term history curve as used here designates a plot of the variation of the deflection of a mass as a function of time. The bridge considered is characterized by the following values of parameters: $\frac{l_1}{l_2} = 0.90$, $\frac{a}{l_2} = 0.20$. The speed parameter α is equal to 0.1035, which corresponds to about 69 mph in an actual bridge-vehicle system. The above numerical values of the parameters were chosen for presentation herein because of the distinctiveness of the dynamic effects that they produced.

Plotted in each figure are both the static and the dynamic deflections as a function of $\tau = \frac{vt}{2L}$. The variable τ may be regarded as a dimensionless measure of time, or a dimensionless measure of the location of the moving force (the force is assumed to move from the left to the right).

During the movement of the load across the bridge the dynamic deflection as well as the static deflection of a given mass changes. The dynamic effect shows itself in the form of oscillations superposed on the static deflection curve.

It may be noted that in all the history curves the dynamic effects are relatively small when the load is on the first portion of the bridge, that is, on the left side-span and left cantilever arm. As soon as the load crosses the left or first hinge the vibrations start to grow larger in amplitude.

In general, the largest amplitude of oscillation occurs when the load is on the right side-span. This behavior had been noted in experiments (1) and it was explained by the fact that before the load reached the right side-span, this span was already excited to motion by the load moving on the other spans. The general features of the history curves mentioned in the preceding are somewhat less marked for m_3 (the mass at the center of the suspended span) than for the other masses.

The dynamic oscillations are not entirely periodic but in nearly all the history curves one can identify sets of waves that possess rather distinct periods. The fundamental and third natural period of vibration can be noticed in the history curve for m_3. An examination of the normal modes as given in Fig. 7 shows that the second and fourth modes should be absent in the response curve of m_3, since it happens to be on a node-point of these modes. In all the history curves, except that for m_3, there can be found distinct trains of waves having periods that lie between the fundamental and second natural period. The average period of such waves is approximately equal to $0.0450 \frac{2L}{v}$, which is close to the second period T_2 ($0.0352 \frac{2L}{v}$) than is to the fundamental period T_1 ($0.0589 \frac{2L}{v}$).

The fourth or the fifth mode appears in a few locations, particularly near the middle of Figs. 8 and 9. It is impracticable to try to distinguish between these two modes, because in this particular case they are very close to each other. The contribution of these two modes is, however, somewhat insignificant. The response of the structure is essentially dominated by the first, second and, to a lesser degree, the third mode. It should be born in mind, however, that this judgment is based on one example. More data are needed to allow one to draw general conclusions concerning the relative contributions of the various modes.

The oscillations of m_1 (the mass at the center of the left side-span) and m_2 (the mass at the left hinge) in many instances have a phase difference of 180 degrees. The same phenomenon exists in the case of m_4 (the mass at the right hinge) and m_5 (the mass at the center of the right side-span). It may be observed from Fig. 7 that such phase differences exist only in the first three modes of vibration.

4. 3. Spectrum Curves with Respect to α

4.3.1. General

While the complete history curve for a particular mass gives the detailed picture of the behavior of that mass at a specific value of the load speed (or α), the most significant point on a history curve is obviously its maximum ordinate, or the maximum dynamic deflection. The ratio of the maximum dynamic deflection to the maximum static deflection on a history curve is called the "maximum amplification factor with respect

to τ," and will be denoted by the symbol $(MAF)_\tau$. There is a $(MAF)_\tau$ corresponding to a given value of α. A plot of $(MAF)_\tau$ against α is referred to as a "spectrum curve with respect to α," or simply, "spectrum curve."

For this study spectrum curves with respect to α have been obtained for the following range of parameters: α from 0.0225 to 0.1125 at intervals of 0.0045 (corresponding to approximately 15 mph to 75 mph at intervals of 3 mph); $\frac{l_1}{l_2}$ from 0.50 to 1.90 at intervals of 0.20; and for three values of $\frac{a}{l_2}$, 0.10, 0.20 and 0.40.

Representative spectrum curves are presented in Figs. 13 through 18. A common characteristic to all these curves is their undulating patterns. This pattern has been noted in the case of simple span bridges (2). In fact the general shapes of the curves for m_1, m_2, and m_3 bear a distinct resemblance to those for simple spans, the corresponding characteristics being the increaseing "amplitudes" and "periods" of the undulations. The general appearance of the curves for m_4 and m_5 resembles less those for simple spans. However, all curves do show the general trend of increasing $(MAF)_\tau$ as α is increased. More detailed interpretation of the data will be presented in the following.

4.3.2. Comparison of Spectrum Curves for m_1 and m_5

It is of interest to compare the spectrum curves for m_1 and m_5 because they are symmetrically located with respect to the center of the bridge. For the majority of cases examined, the spectrum curve for m_5

generally lies above that for m_1, signifying a larger dynamic effect for m_5 than for m_1. This situation is illustrated in Fig. 13. In these cases the maximum dynamic deflection of m_1 generally occurs when the moving load is near the middle of the left side-span. The time interval between the initiation of the motion of this mass and the occurrence of the maximum dynamic deflection is relatively small. On the other hand, in the case of m_5 the maximum dynamic deflection does not occur until the moving load has traveled a great length on the bridge. Thus on the basis of the duration of excitation, it is reasonable to expect that the dynamic effect for m_5 would be larger than that for m_1.

There are, however, some exceptions to the feature mentioned in the preceding. For $\frac{l_1}{l_2}$ = 0.50 to 1.10 and large values of the $\frac{a}{l_2}$ ratio the spectrum curves for m_1 and m_5 are located quite close to each other, intersecting at several points. This is illustrated in Fig. 14. An explanation is given as follows: In the above-mentioned range of parameters the cantilever arm is relatively long. This causes the maximum dynamic deflection of m_1 to take place after the moving load has crossed the left-side-span and is near the left hinge. Thus the maximum dynamic deflection of m_1 is associated with a longer duration of excitation and consequently a larger magnitude.

4.3.3. Comparison of Spectrum Curves for m_2 and m_4

Presented in Fig. 15 ($\frac{l_1}{l_2}$ = 0.90, $\frac{a}{l_2}$ = 0.10) and Fig. 16 ($\frac{l_1}{l_2}$ = 0.50, $\frac{a}{l_2}$ = 0.10) are typical spectrum curves for m_2 and m_4.

Comparisons of spectrum curves for m_2 and m_4 indicate similar relationships between m_2 and m_4 to those between m_1 and m_5. Whenever the maximum dynamic deflection of m_2 takes place as the load is traversing the left side-span, the spectrum curve of m_4 lies above that of m_2 (see Fig. 15). If the maximum dynamic deflection occurs when the load is near the left hinge, the two spectrum curves are close to each other (see Fig. 16). This feature can be explained, as for the case of m_1 and m_5, in terms of the dependence of the dynamic effects on the duration of excitation.

4.3.4. Spectrum Curves for m_3

Typical spectrum curves for m_3 are given in Fig. 17 ($\frac{l_1}{l_2} = 0.50$, $\frac{a}{l_2} = 0.10$) and Fig. 18 ($\frac{l_1}{l_2} = 1.30$, $\frac{a}{l_2} = 0.20$).

The resemblance of the curve in Fig. 17 to a typical spectrum curve for the mid-span deflection of a simply supported beam (2) is quite striking. The reason is thought to be that for the structure considered in this figure the suspended span is long relative to both the side span and the cantilever arm. It follows that the masses on the latter spans are small as compared to m_3 and hence they have a relatively small influence on its motion. On the other hand, the stiffness of the side-span and the cantilever arm is relatively large because of their short lengths. Under these conditions the center span could be expected to behave essentially as a simply supported beam.

In Fig. 18 it may be noted that the spectrum curve for the structure involved is substantially different from that for a simply supported span.

This may be explained by the fact that the structure concerned has a long side-span. Hence the conditions related in the preceding paragraph are essentially reversed. In this case the side-spans could have a fairly large influence on the behavior of the suspended span from the standpoint of both the inertia forces and stiffness. Consequently, the suspended span no longer behaves like a simply supported beam.

In passing, it may be noted that Figs. 13, 16, and 17 constitute a complete set of spectrum curves for the bridge with $\frac{l_1}{l_2} = 0.50$ and $\frac{a}{l_2} = 0.10$.

4.3.5. Negative Amplification Factors

Whenever the maximum dynamic and static deflections do not occur when the load is on the same span, negative amplification factors result (see Tables 2b and 2c). This follows from the fact that the sign of the maximum dynamic deflection is opposite to that of the static. For example, in the case of m_1, while the maximum static deflection occurs when the load is on the left side-span, the maximum dynamic deflection may take place when the load is on the left cantilever arm, or vice versa.

4.4. Maximum Response

The maximum ordinate of each of the spectrum curves obtained for this study is listed in Tables 2a, 2b and 2c. The values of τ and α at which this maximum occurs are also given. For convenience the data in these tables are also presented graphically in Figs. 19 through 23.

Table 2a. Maximum amplification factors with respect to τ and α, for $\frac{a}{\ell_2} = 0.10$

ℓ_1 / ℓ_2		Maximum A. F. Point m_1	Point m_2	Point m_3	Point m_4	Point m_5
	at	1.14	1.28	1.14	1.20	1.37
0.50	τ =	.0560	.1410	.2255	.3660	.4415
	α =	.1125	.1125	.1125	.0900	.0990
	at	1.16	1.17	1.13	1.39	1.36
0.70	τ =	.0675	.0695	.2545	.4335	.4355
	α =	.1125	.1125	.0855	.0945	.0945
	at	1.13	1.13	1.10	1.49	1.41
0.90	τ =	.0795	.0825	.2540	.4080	.4110
	α =	.1125	.1125	.1125	.1080	.1080
	at	1.15	1.19	1.22	1.31	1.27
1.10	τ =	.0865	.0940	.2470	.4065	.4200
	α =	.1035	.1125	.1125	.0945	.0720
	at	1.17	1.20	1.13	1.19	1.23
1.70	τ =	.1000	.1130	.2550	.3930	.4205
	α =	.0945	.1080	.0990	.0810	.1125
	at	1.17	1.20	1.13	1.20	1.23
1.90	τ =	.1005	.1160	.2545	.4005	.4190
	α =	.0900	.1035	.0630	.0900	.1080

Table 2b. Maximum amplification factors with respect to τ and α, for $\frac{a}{\ell_2} = 0.20$

ℓ_1/ℓ_2		Maximum A. F. Point m_1	Point m_2	Point m_3	Point m_4	Point m_5
	at	1.25	1.19	1.08	1.23	1.28
0.50	τ =	.1570	.1560	.2495	.3560	.3630
	α =	.1080	.1125	.0675	.0990	.1035
	at	-1.12*	1.20	1.06	1.20	1.32
0.70	τ =	.1710	.1690	.2540	.3430	.4470
	α =	.0945	.1125	.0720	.0945	.0945
	at	1.06	1.27	1.10	1.13	1.35
0.90	τ =	.0720	.1790	.2420	.3325	.4490
	α =	.0450	.0990	.1035	.0810	.1035
	at	1.12	1.19	1.24	-1.20*	1.27
1.10	τ =	.0800	.1870	.2490	.4065	.4180
	α =	.0945	.1125	.1125	.1125	.0810
	at	1.15	1.20	1.19	1.56	1.43
1.30	τ =	.0875	.0995	.2530	.4145	.4125
	α =	.0990	.1125	.1125	.1125	.1125
	at	1.17	1.20	1.19	1.41	1.30
1.50	τ =	.0930	.1035	.2525	.3925	.4130
	α =	.0990	.1080	.0855	.0900	.1080
	at	1.17	1.21	1.15	1.28	1.25
1.70	τ =	.0945	.1115	.2495	.4070	.4150
	α =	.0945	.1080	.0810	.1125	.0720
	at	1.17	1.21	1.16	1.34	1.34
1.90	τ =	.0995	.1125	.2605	.4165	.4155
	α =	.0945	.1080	.0810	.1125	.1125

*See explanation in the text.

Table 2c. Maximum amplification factors with respect to τ and α, for $\frac{a}{\ell_2} = 0.40$

ℓ_1/ℓ_2		Maximum A. F. Point m_1	Point m_2	Point m_3	Point m_4	Point m_5
	at	1.24	1.22	1.13	1.20	1.24
0.50	τ =	.1750	.1780	.2500	.3220	.3465
	α =	.1125	.1125	.0720	.1125	.0810
	at	1.24	1.19	1.13	1.25	1.31
0.70	τ =	.1855	.1865	.2625	.3370	.3385
	α =	.1080	.1125	.0900	.0855	.0855
	at	1.28	1.20	1.17	1.22	1.30
0.90	τ =	.1950	.1940	.2570	.3230	.3320
	α =	.1035	.1080	.0765	.0810	.0900
	at	1.27	1.20	1.16	1.27	1.39
1.10	τ =	.2025	.1995	.2595	.3200	.3215
	α =	.1080	.1125	.0855	.0855	.0855
	at	-1.19*	1.17	1.20	1.23	1.37
1.30	τ =	.2045	.2035	.2710	.2985	.4025
	α =	.0900	.0945	.0990	.1125	.0900
	at	1.10	1.20	1.18	1.27	1.43
1.50	τ =	.0815	.2085	.2520	.3000	.4180
	α =	.0810	.1125	.0765	.1125	.0765
	at	1.13	1.25	1.20	1.27	1.49
1.70	τ =	.0860	.2105	.2600	.3005	.4025
	α =	.0855	.1125	.0810	.1125	.1125
	at	1.15	1.28	1.20	-1.36*	1.54
1.90	τ =	.0910	.2135	.2260	.4060	.4055
	α =	.0900	.1125	.1125	.1125	.1125

*See explanation in the text.

Most curves in Figs. 19-23 show no distinct trends. This may be due to insufficient data. It may be noted, however, that curves for m_3, m_4 and m_5 and $\frac{a}{l_2} = 0.40$, generally indicate an increase in dynamic effects with an increase in the values of $\frac{l_1}{l_2}$. Another feature that may be noted from these curves is that the ranges of variation of the maximum amplification factors are larger for m_1, m_4 and m_5 than for m_2 and m_3.

The absolute maximum amplification factor for each mass (maximum A. F. with respect to τ, a, $\frac{l_1}{l_2}$ and $\frac{a}{l_2}$) is listed below:

TABLE 3. Absolute maximum A. F.

Mass-point	Absolute maximum A.F.	$\frac{l_1}{l_2}$	$\frac{a}{l_2}$
1	1.28	0.90	0.40
2	1.28	1.90	0.40
3	1.24	1.10	0.20
4	1.56	1.30	0.20
5	1.54	1.90	0.40

From the above table it may be noted that the absolute maximum A. F. does not vary appreciably among m_1, m_2 and m_3. However, it is much greater for m_4 and m_5. The value of the absolute maximum A. F. of 1.56 for m_4 and 1.54 for m_5 must be considered to be striking under the given loading condition, i. e., a constant moving force.

V. SUMMARY AND CONCLUDING REMARKS

An analytical study of the dynamic response of three-span cantilever bridges has been presented. The major findings of the study are summarized and discussed as follows:

1. The dynamic effects in this type of bridges as caused by moving loads can be quite large. The greatest dynamic effect found within the data obtained is 56 per cent larger than the corresponding maximum static effect. This is quite striking, particularly if one considers the fact that the investigation has not included the influence of such factors as the vertical springing motion of the vehicle and the unevenness of the bridge deck surface. The latter factors all tend to increase the dynamic effects of the moving load.

2. The dynamic effects generally increase as the speed of the moving force increases.

3. From a study of a limited number of history curves at different sections of the bridge, it has been found that the major contributions to the dynamic deflection of the bridge come from the participation of the first, second and to a lesser degree the third normal mode of vibration. Response in the 4th and 5th modes is scarce and of relatively minor importance.

4. In general, the dynamic effects are larger for the latter portion of the bridge than for the first portion. This seems to indicate that for a given speed the amount of excitation to which the bridge is subjected increases with the duration of the travel of the moving load on the bridge.

The constant force representation of the moving load may be considered as a preliminary step for an investigation of the dynamic behavior of cantilever bridges. In the author's opinion, future studies should commence with an extension of the present analysis to consider more realistic representations of highway vehicles. For example a vehicle may be idealized as a mass supported by two springs, representing the two axles of a vehicle. In this manner, the vertical bouncing motion and angular pitching motion may be taken into account in the analysis. In addition, for a more comprehensive study of the problem the effect of the unevenness of the bridge deck needs to be accounted for. Last but not the least, for applications to the design of such structures, the dynamic bending moments in the bridge, in addition to the dynamic deflections, should be included in future studies.

LIST OF REFERENCES

1. Wen, R. K. L., "Dynamic Behavior of Cantilever Bridges Under Moving Loads," Progress Report No. 1, Division of Engineering Research, College of Engineering, Michigan State University, February, 1960.

2. Wen, R. K. L., "Dynamic Behavior of Simple Span Highway Bridges Traversed by Two-Axle Vehicles," Civil Engineering Studies, Structural Research Series No. 142, University of Illinois, 1957.

3. Oehler, LeRoy, T., "Vibration Susceptibilities of Various Highway Bridge Types," Journal of the Structural Division, Proceedings of ASCE, July 1957.

4. Huang, T., and Veletsos, A. S., "A Study of Dynamic Response of Cantilever Highway Bridges," Civil Engineering Studies, Structural Research Series No. 206, University of Illinois, 1960.

5. Newmark, N. M., "A Method of Computation of Structural Dynamics," Journal of Engineering Mechanics Division, Proceedings, ASCE, July 1959, pp. 67-94.

6. Konishi, I. and Komatsu, S., "Vibration Behavior of Gerber Beam," Technical Report No. 29, Vol. 6, No. 3, The Engineering Research Institute, Kyoto University, Kyoto, Japan, 1956.

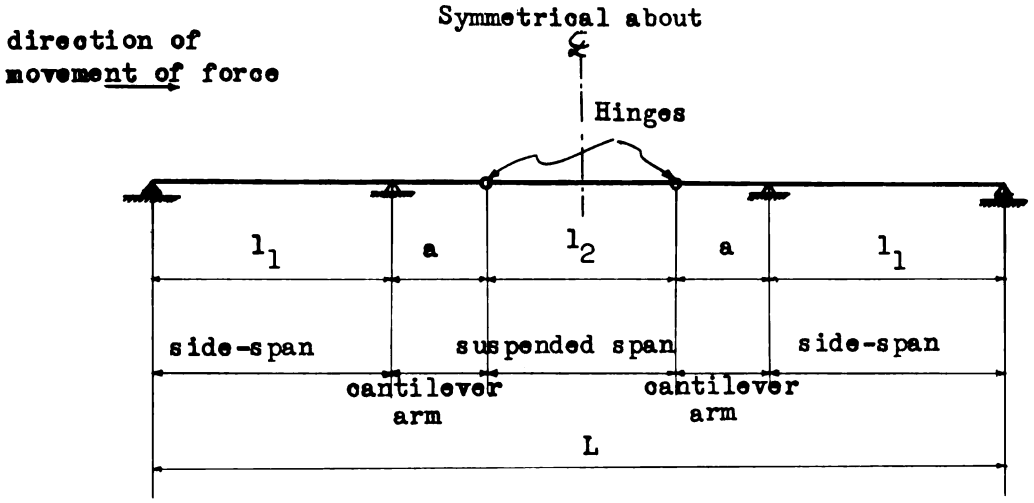

(a) Cantilever bridge type

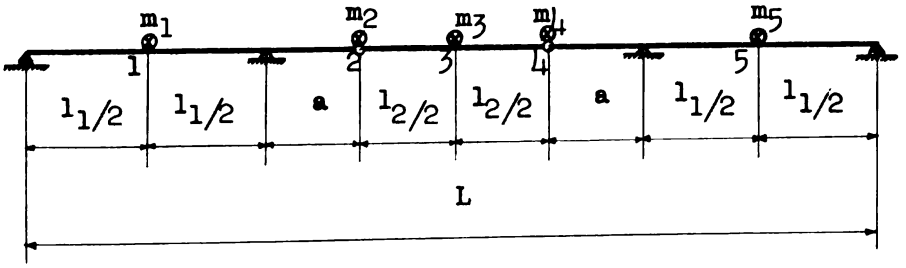

m_b = mass per unit length of beam

$m_1 = m_5 = m_b \left(\frac{l_1}{2}\right)$

$m_2 = m_4 = m_b \left(\frac{l_1}{4} + \frac{a}{2}\right)$

$m_3 = m_b \left(\frac{l_2}{2}\right)$

(b) Concentrated point masses

FIG. 1 - SYSTEM CONSIDERED

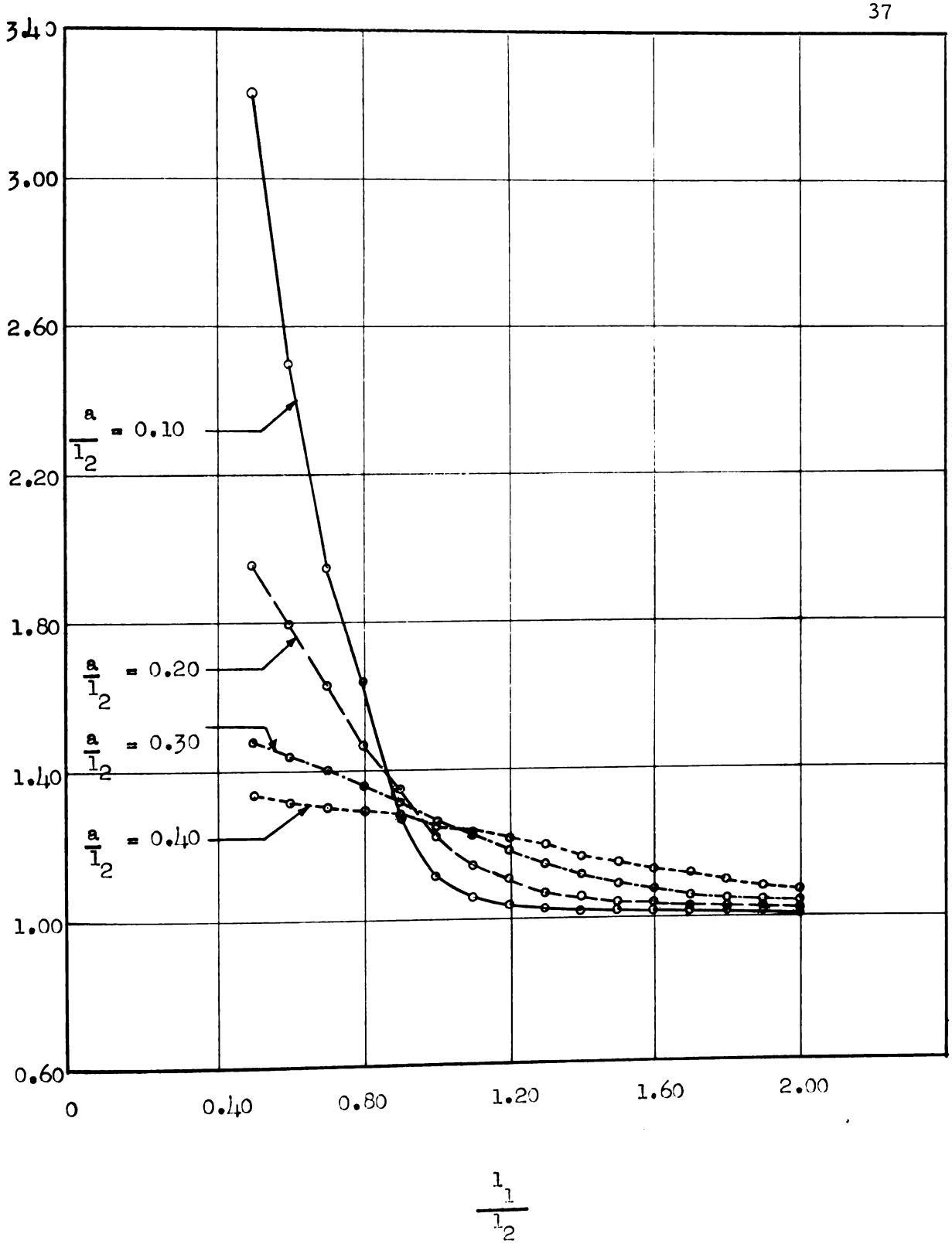

Fig. 2 - Relations between T_1 and T_2

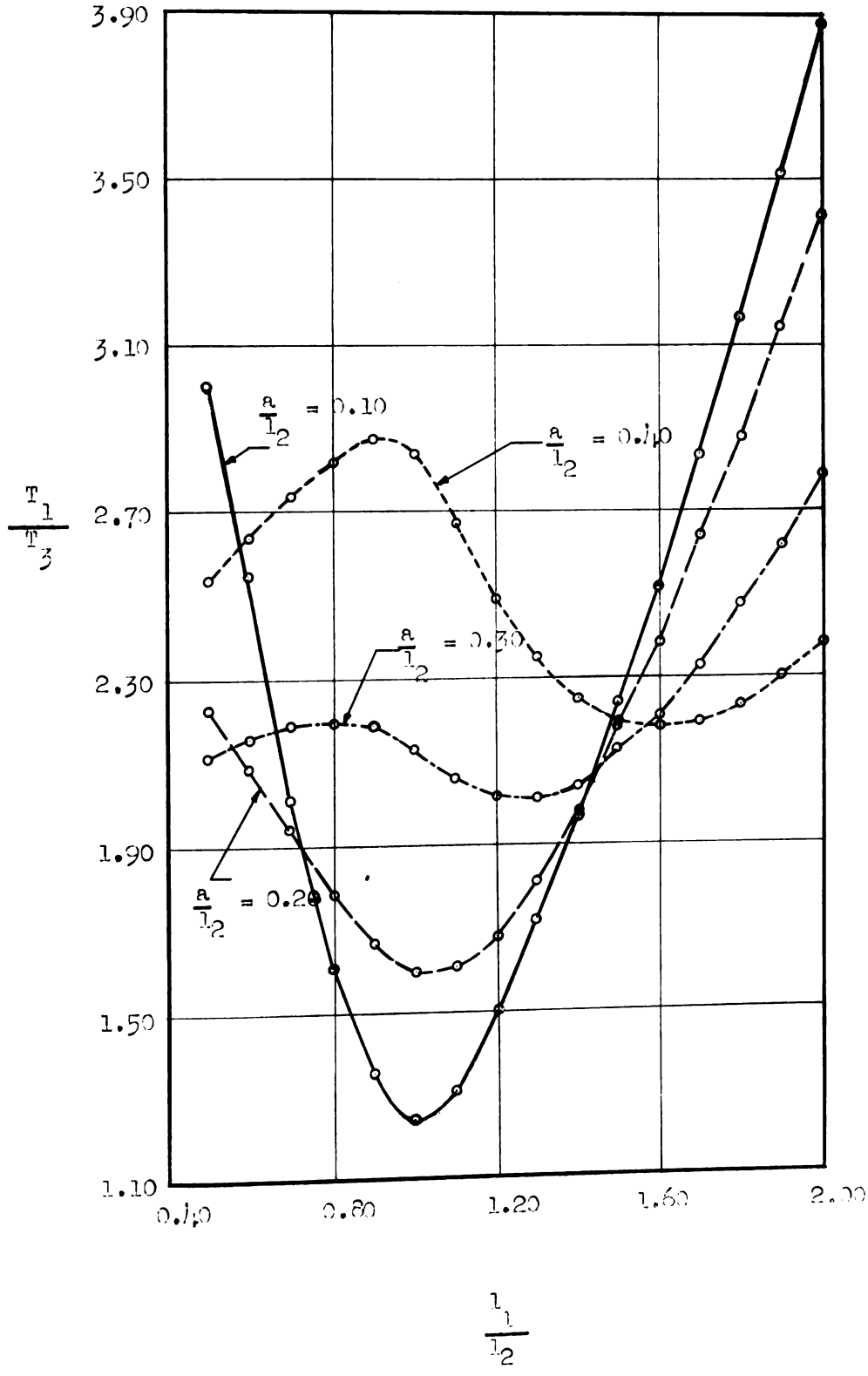

Fig. 3 - Relations between T_1 and T_3

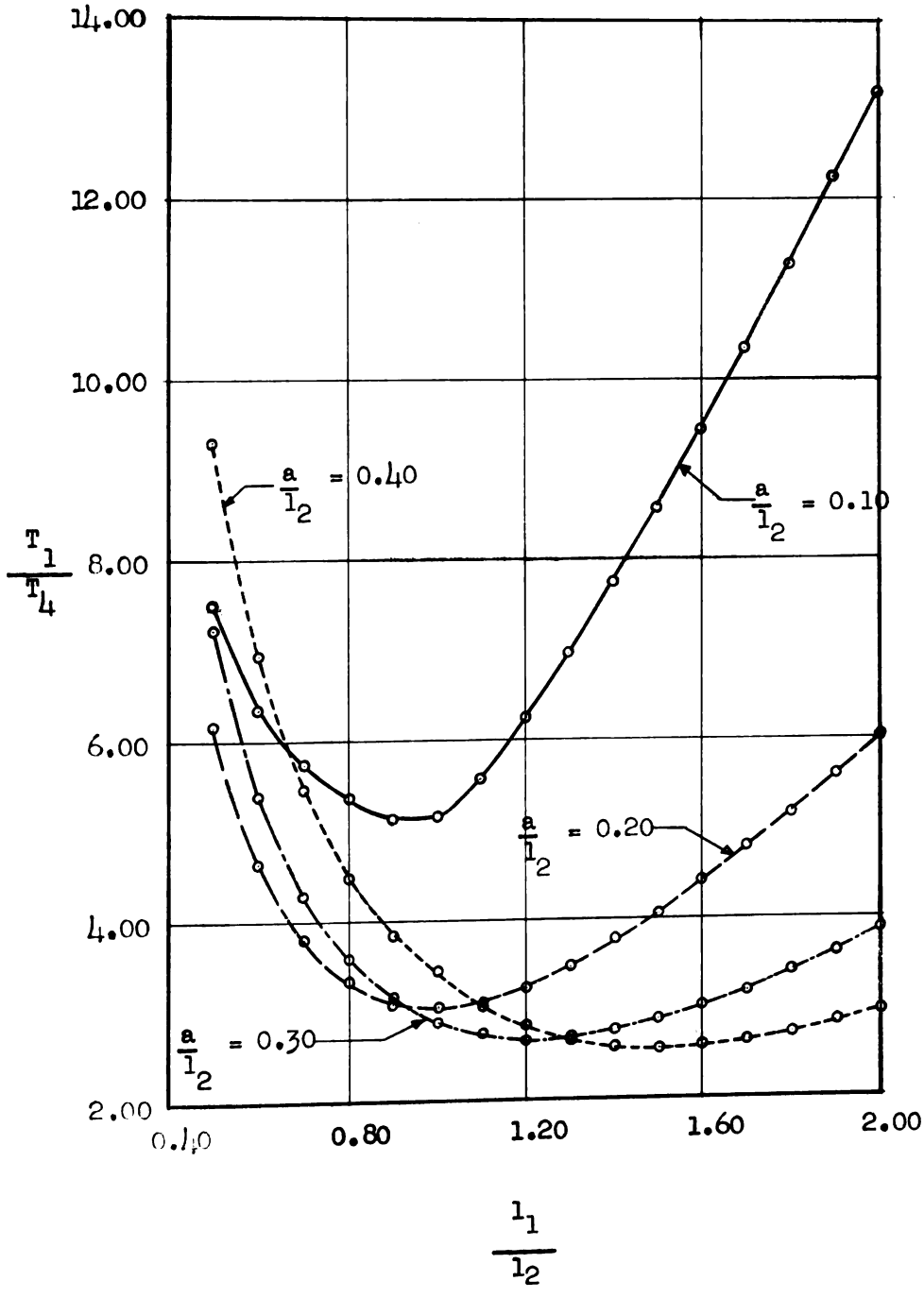

Fig. 4 - Relations between T_1 and T_4

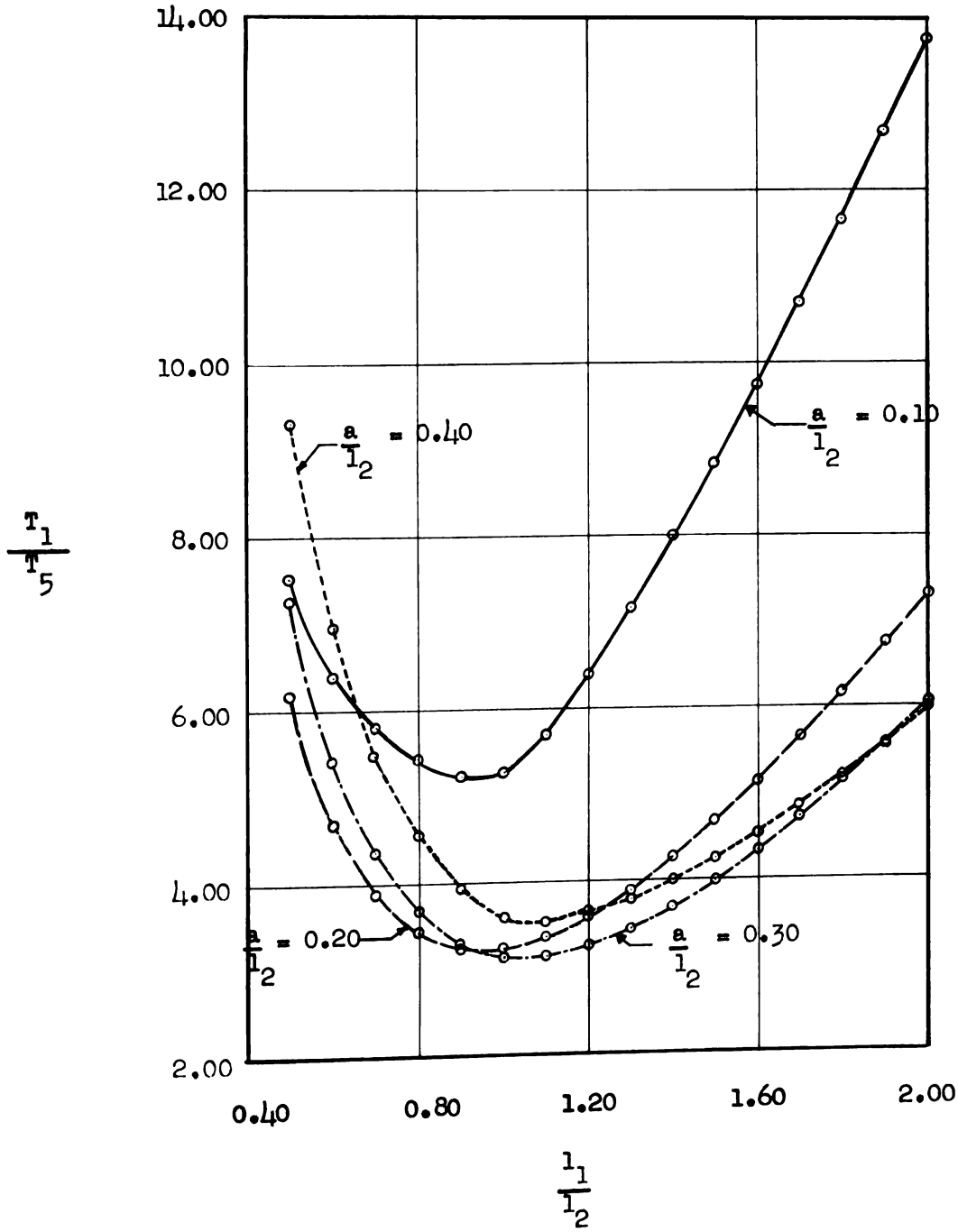

Fig. 5 - Relations between T_1 and T_5

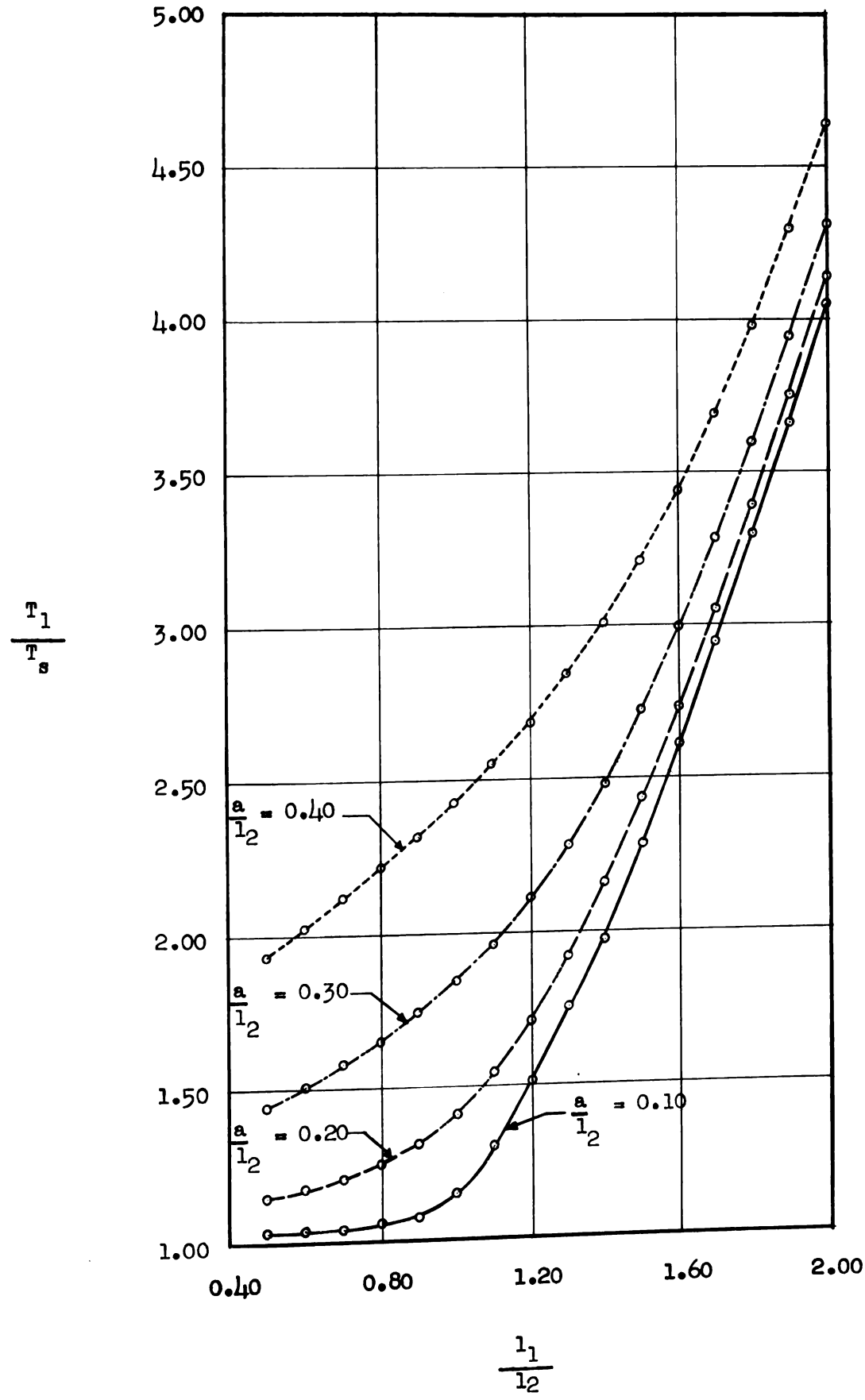

Fig. 6 - Relations between T_1 and T_s

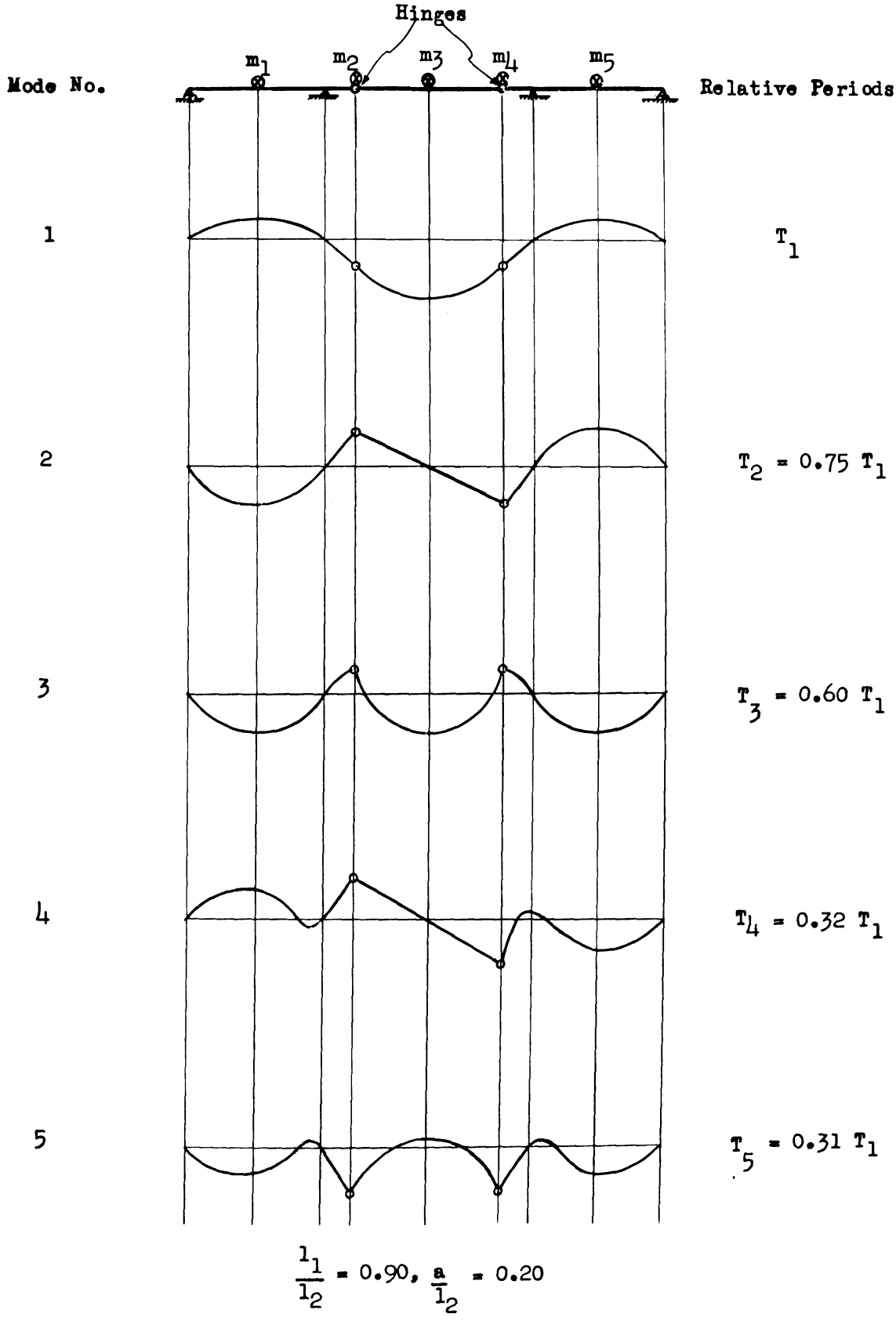

Fig. 7 - Normal modes of vibration

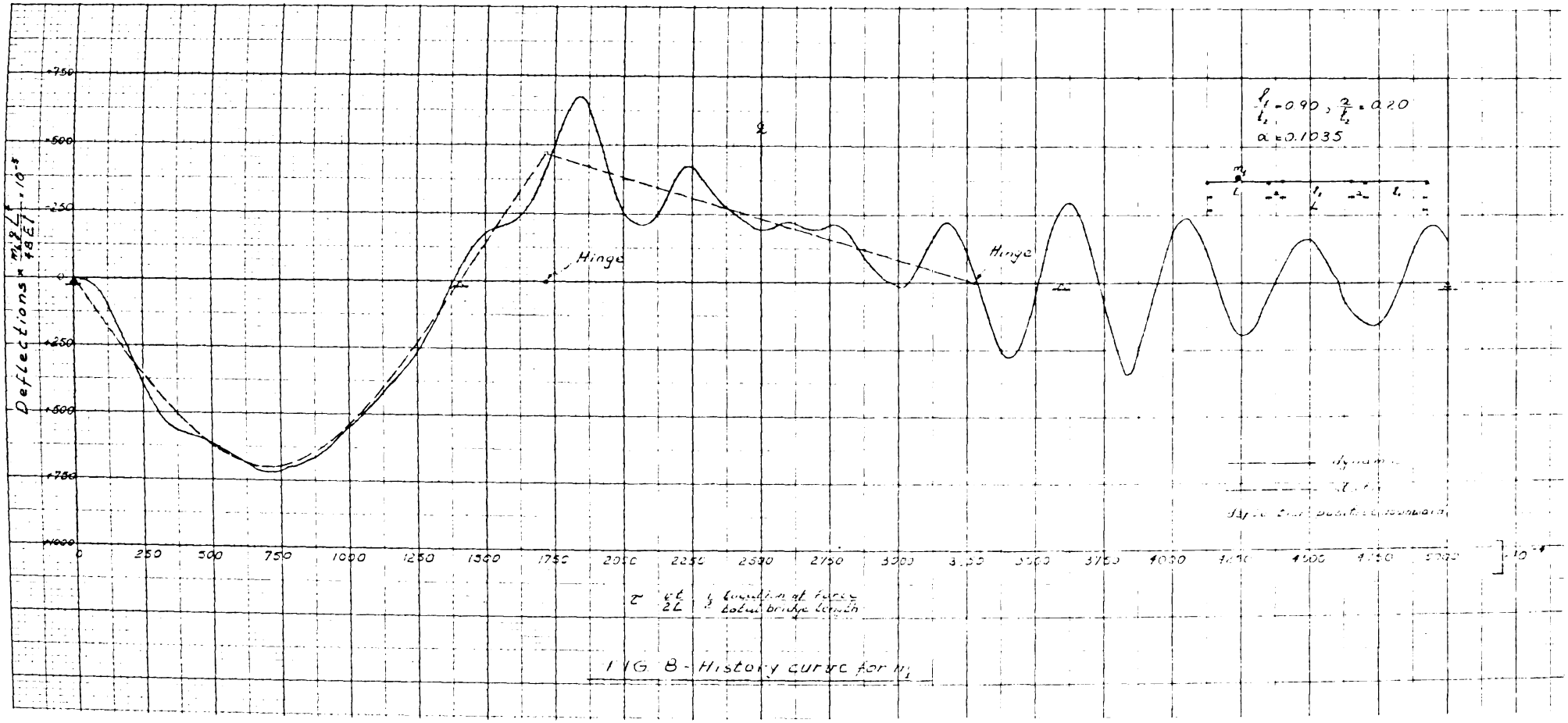

FIG. 8 - History curve for M_1

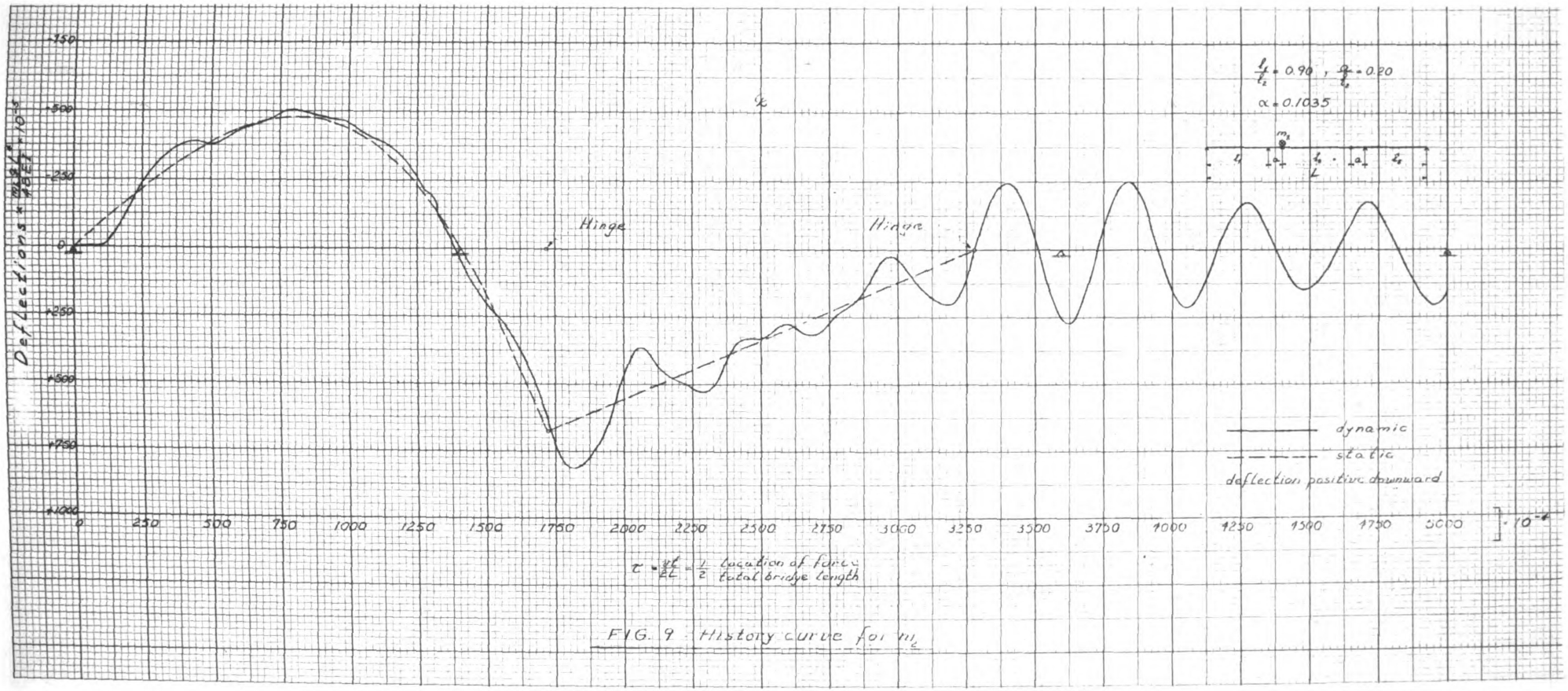

FIG. 9 History curve for w_2

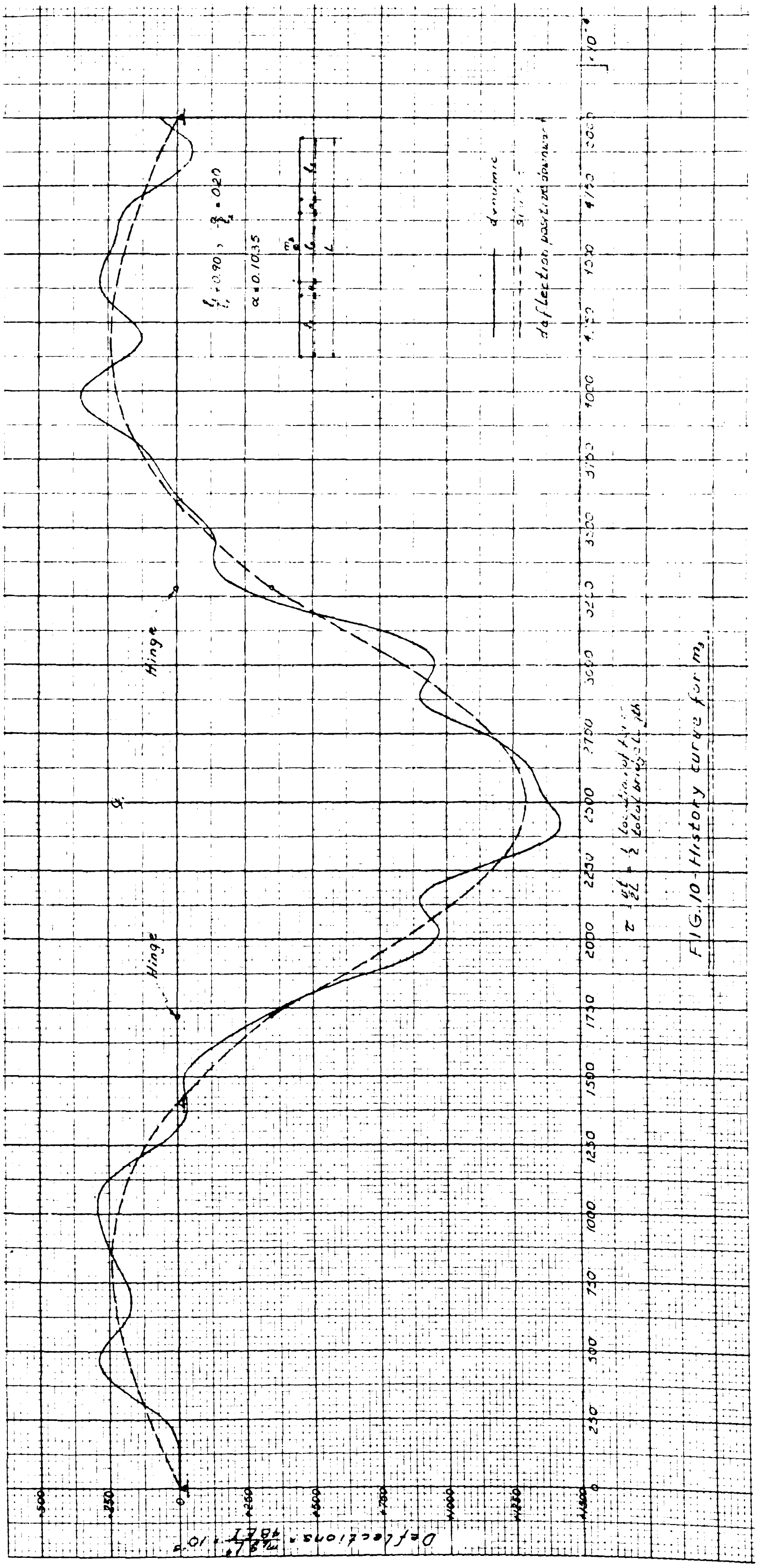

FIG. 10-History curve for m_3

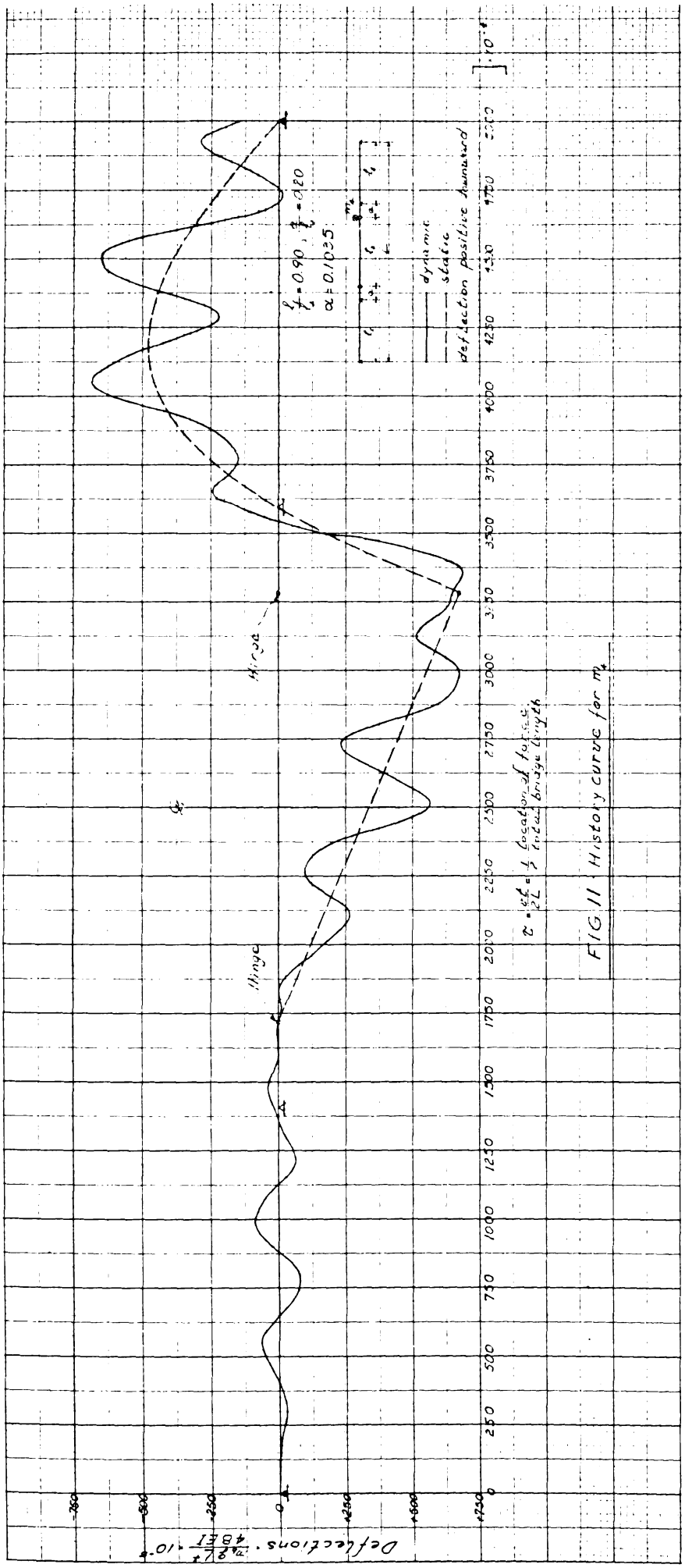

FIG 11 History curve for m_4

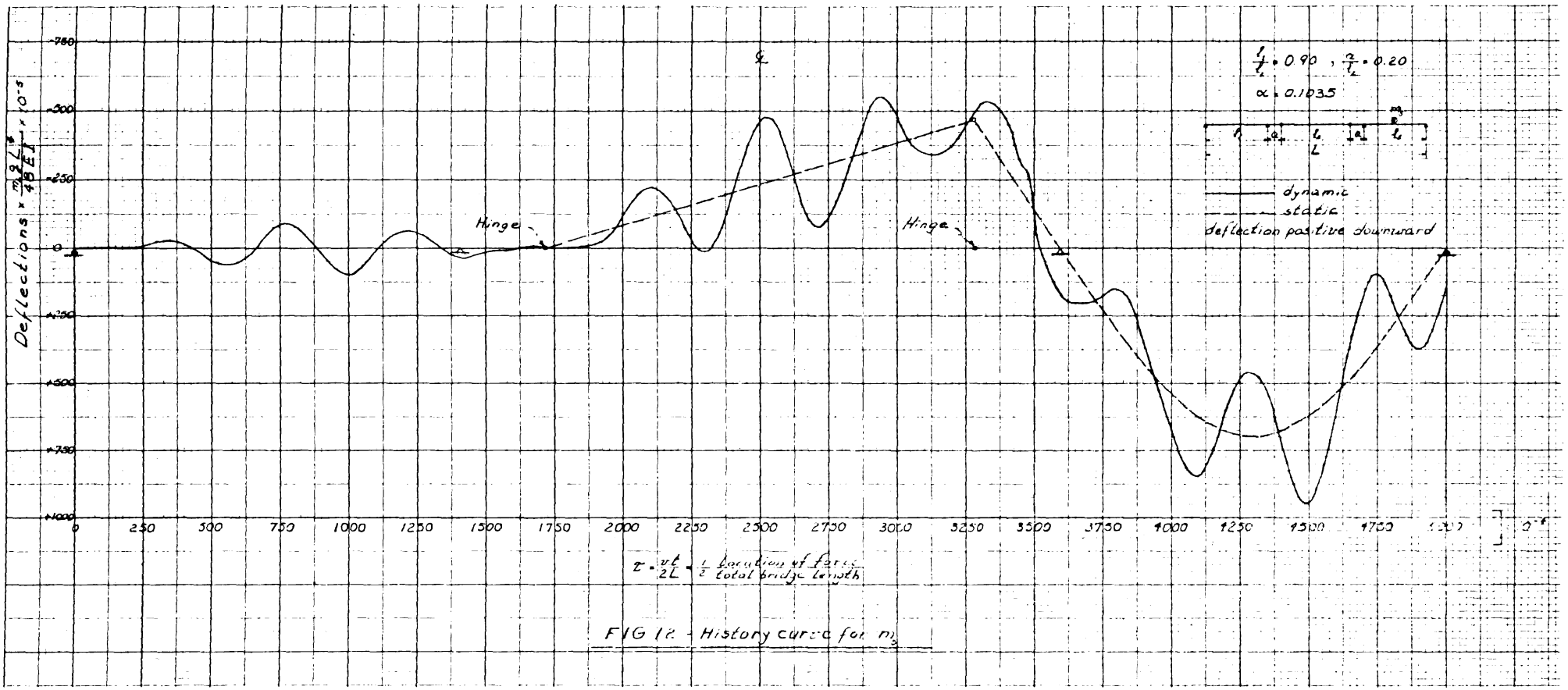

FIG 12 - History curves for m_2

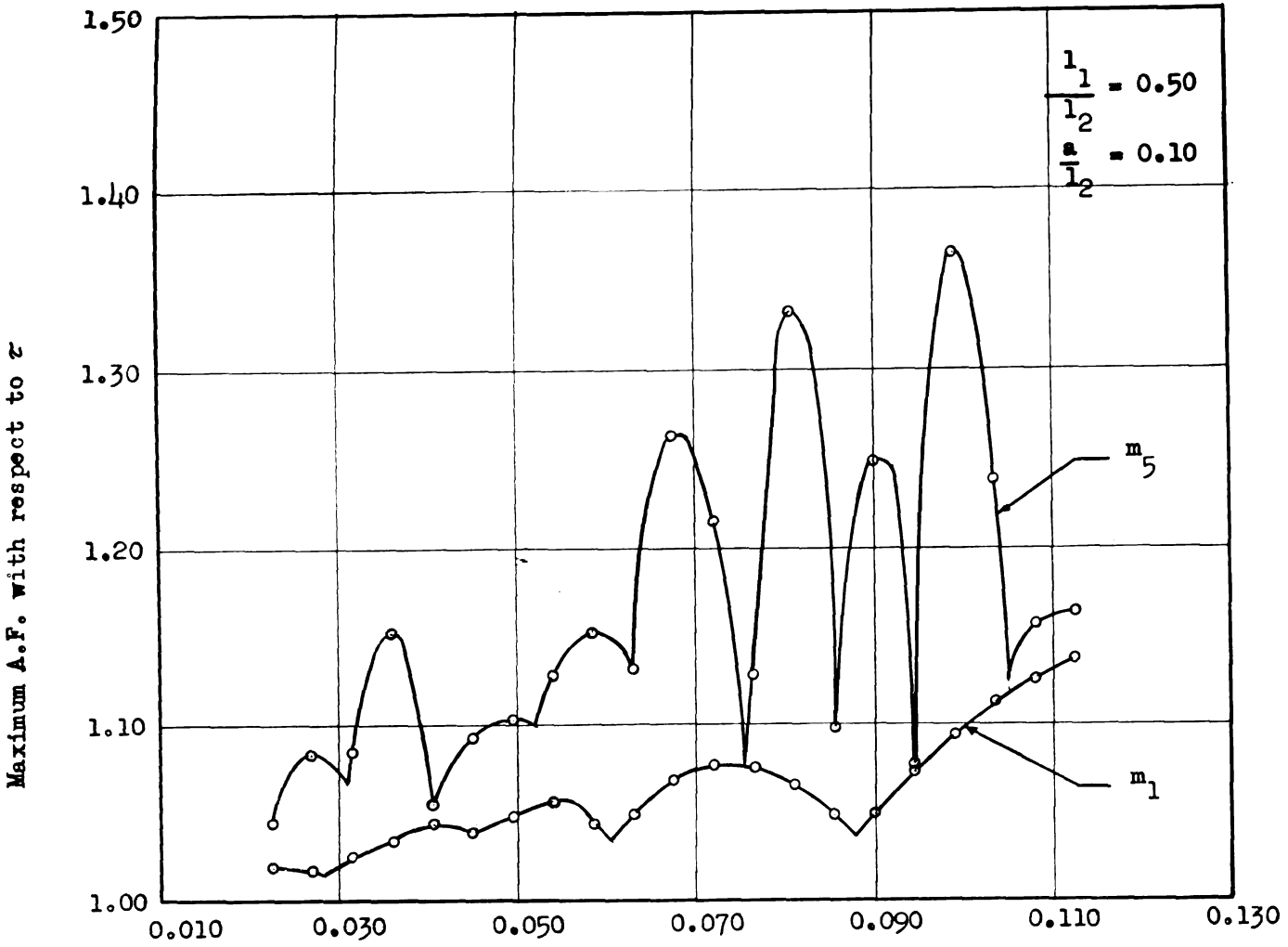

Fig. 13 - Spectrum curves for m_1 and m_5 ($\frac{l_1}{l_2} = 0.50$, $\frac{a}{l_2} = 0.10$)

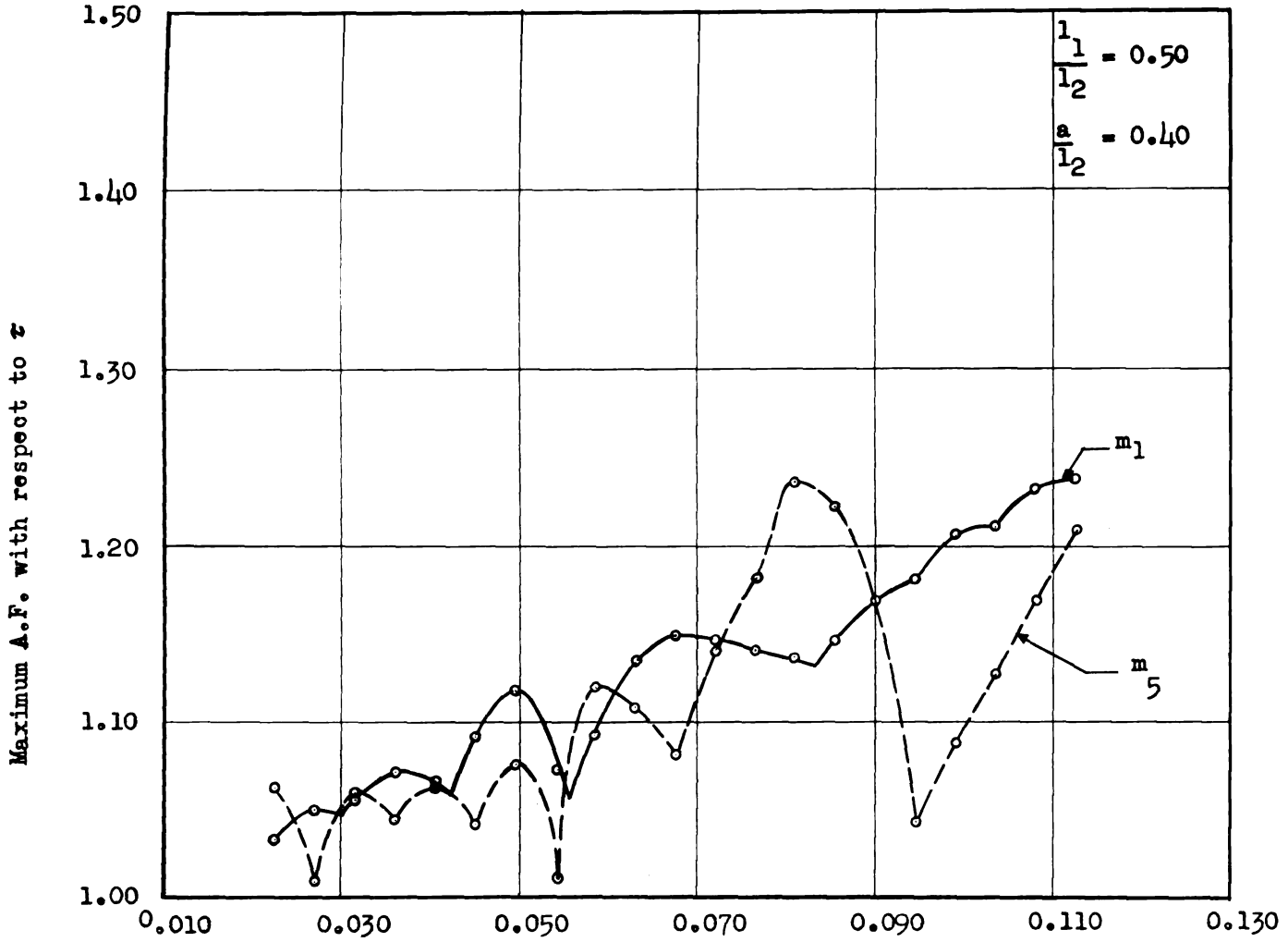

Fig. 14 - Spectrum curves for m_1 and m_5 ($\frac{l_1}{l_2}$ = 0.50, $\frac{a}{l_2}$ = 0.40)

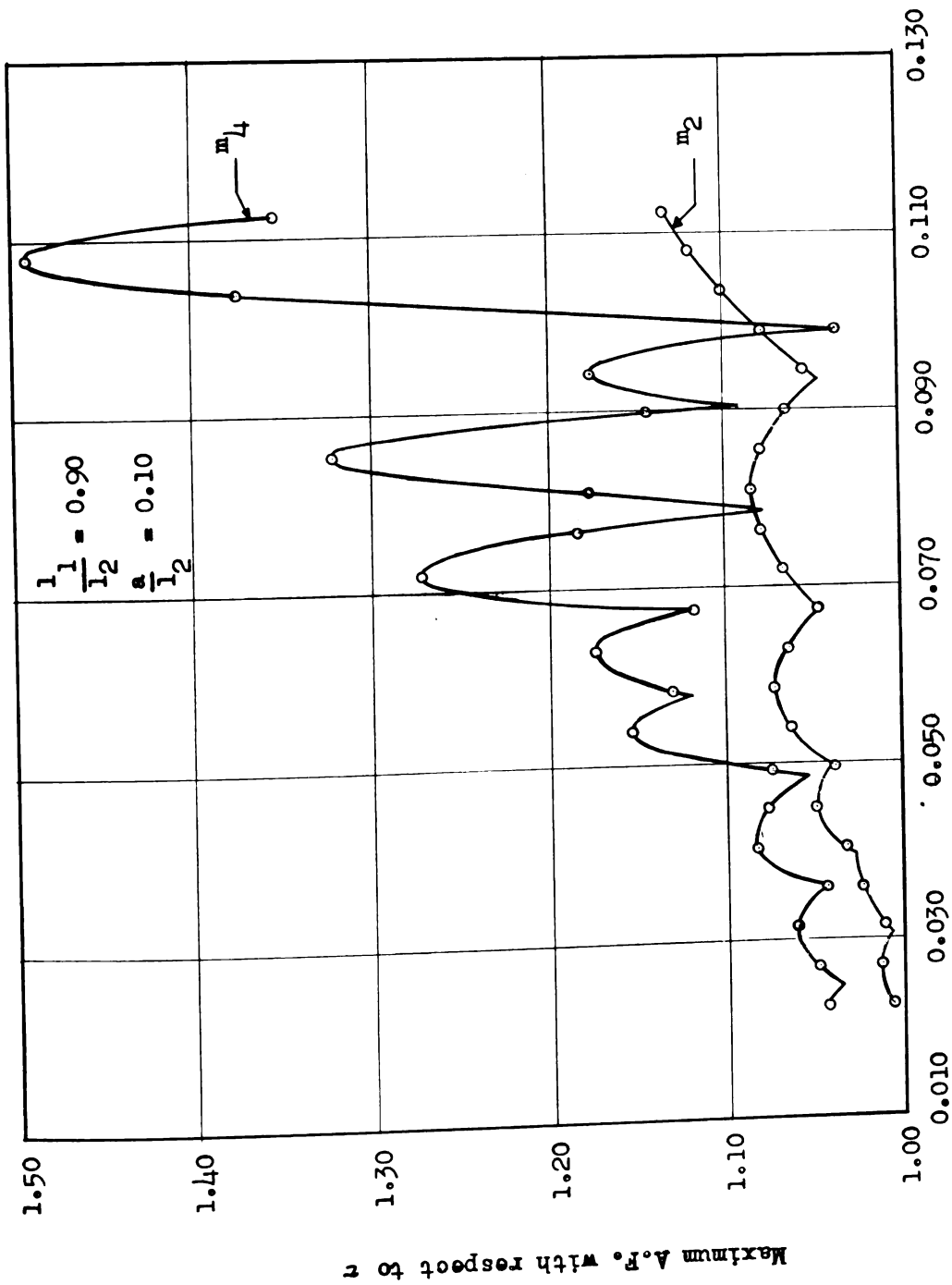

Fig. 15 - Spectrum curves for m_2 and m_4 ($\frac{l_1}{l_2} = 0.90$, $\frac{a}{l_2} = 0.10$)

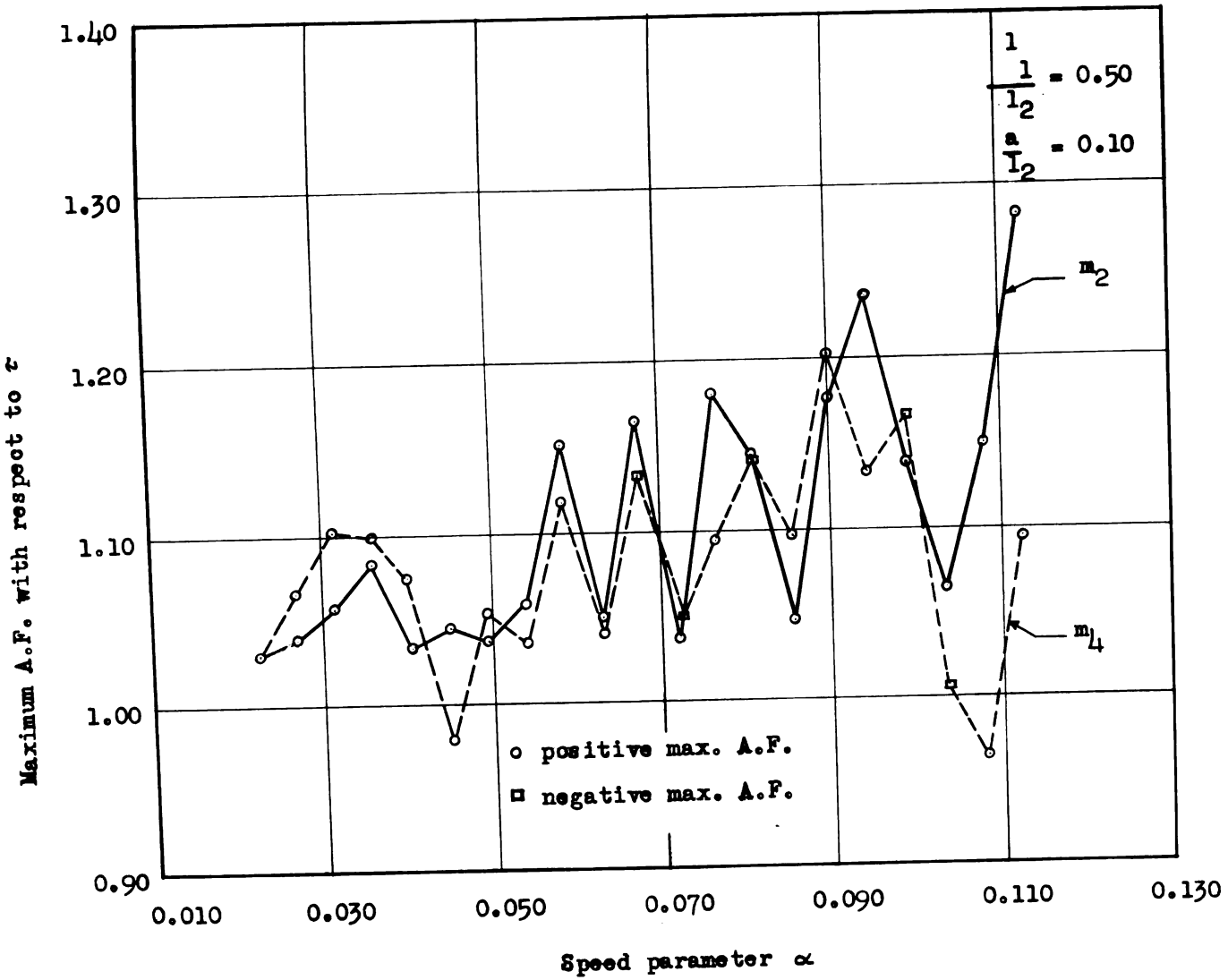

Fig. 16 - Spectrum curves for m_2 and m_4 ($\frac{l_1}{l_2} = 0.50$, $\frac{a}{l_2} = 0.10$)

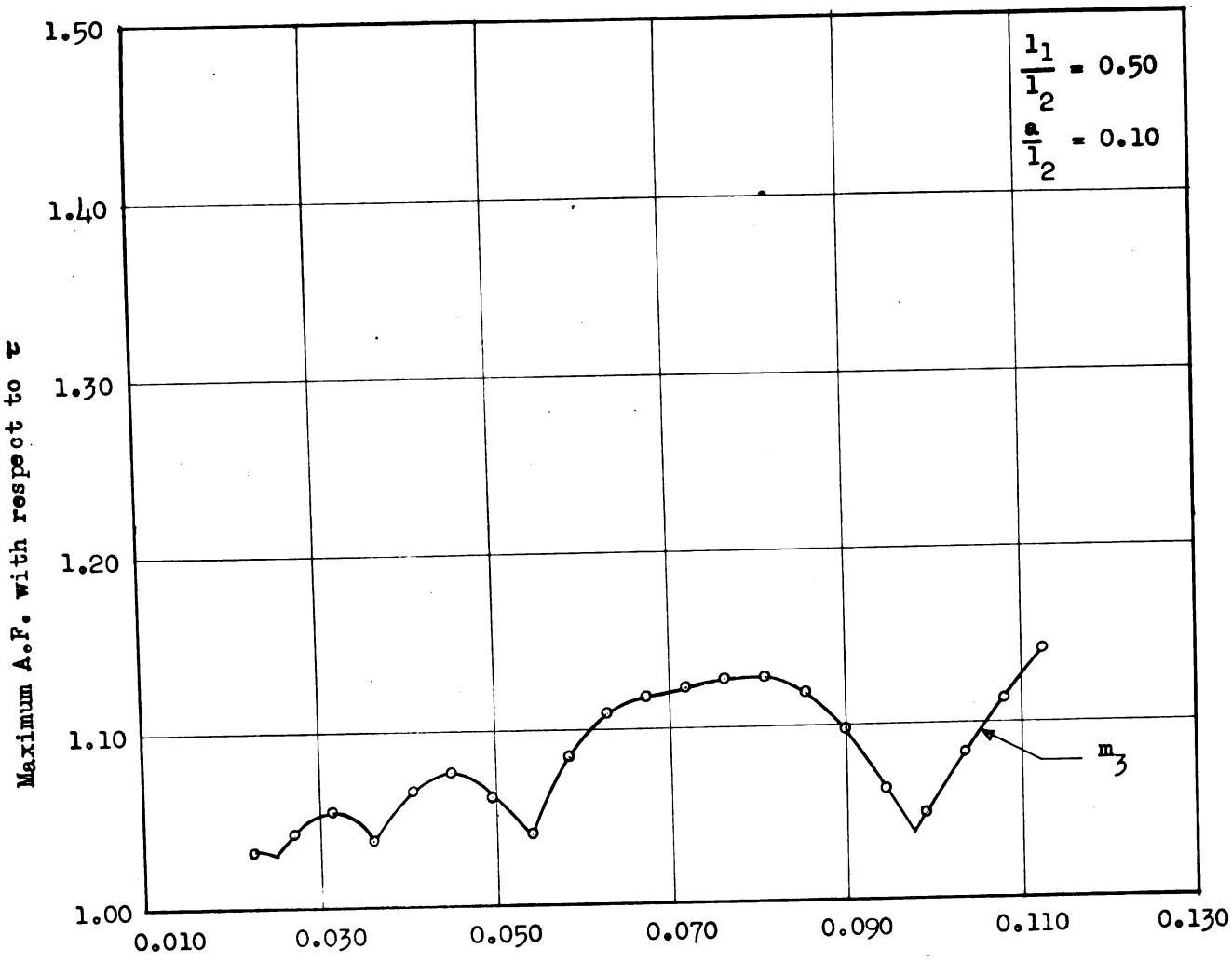

Fig. 17 - Spectrum curve for m_3 ($\frac{l_1}{l_2} = 0.50$, $\frac{a}{l_2} = 0.10$)

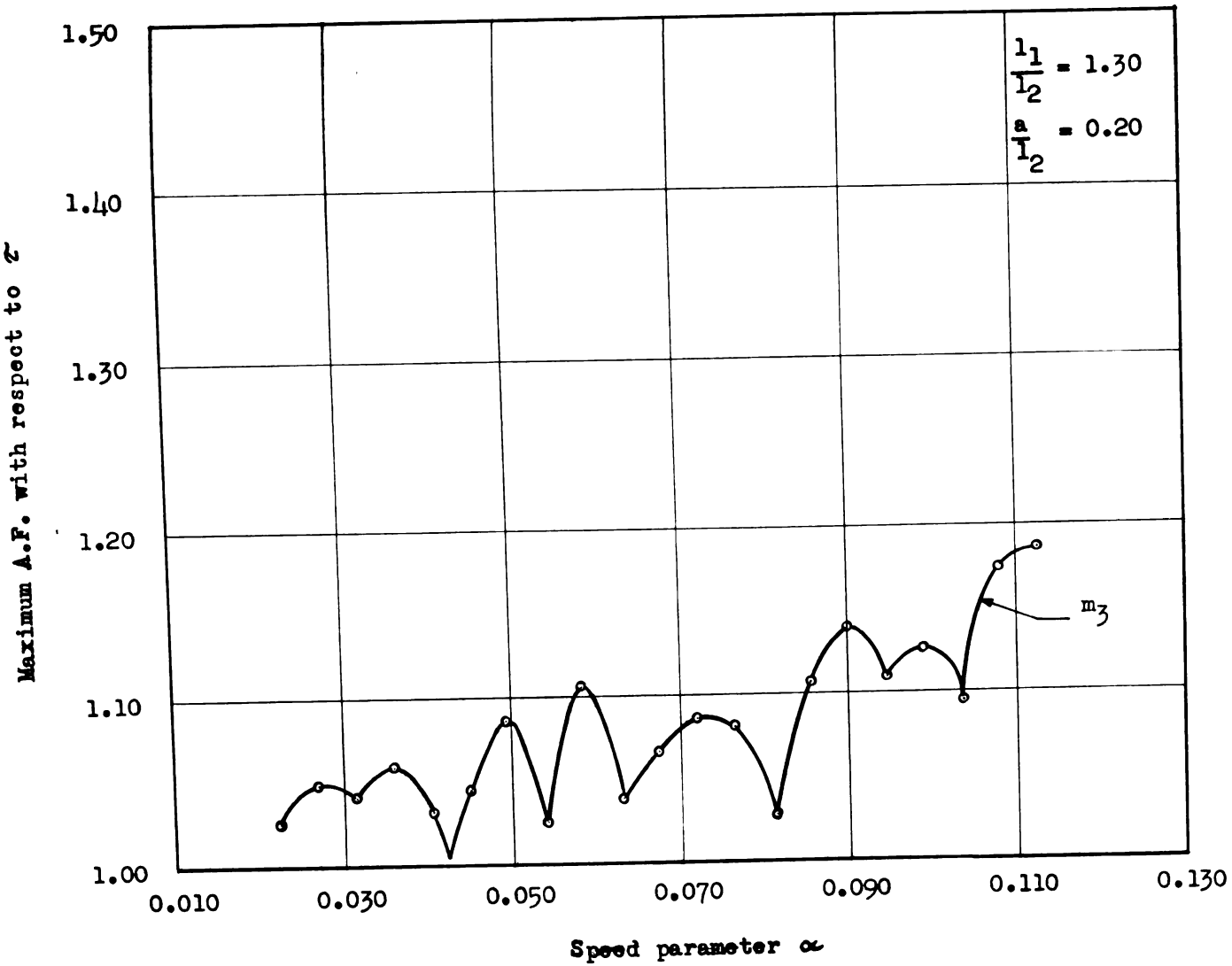

Fig. 18 - Spectrum curve for m_3 ($\frac{l_1}{l_2}$ = 1.30, $\frac{a}{l_2}$ = 0.20)

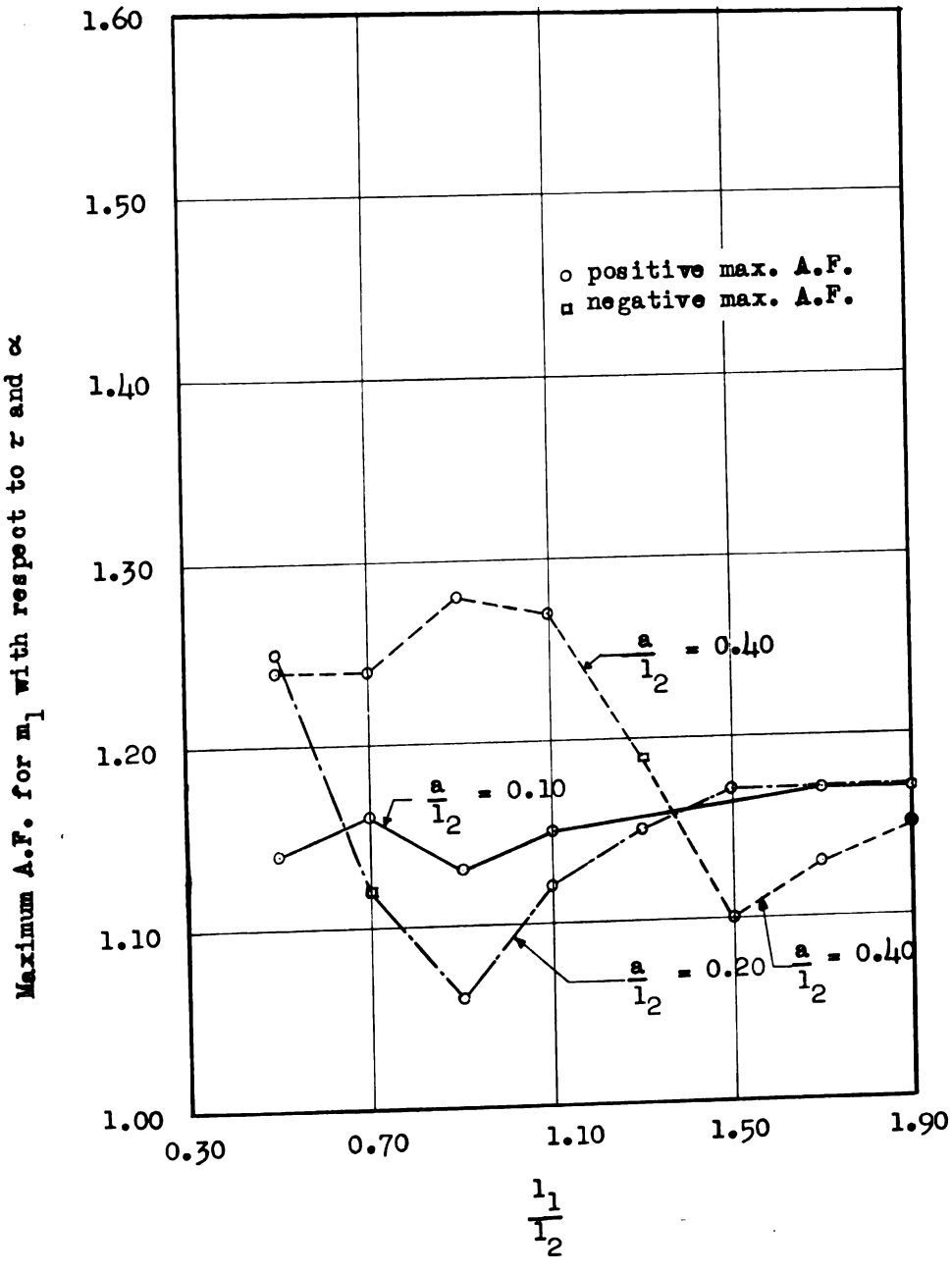

Fig. 19 - Maximum amplification factor for m_1

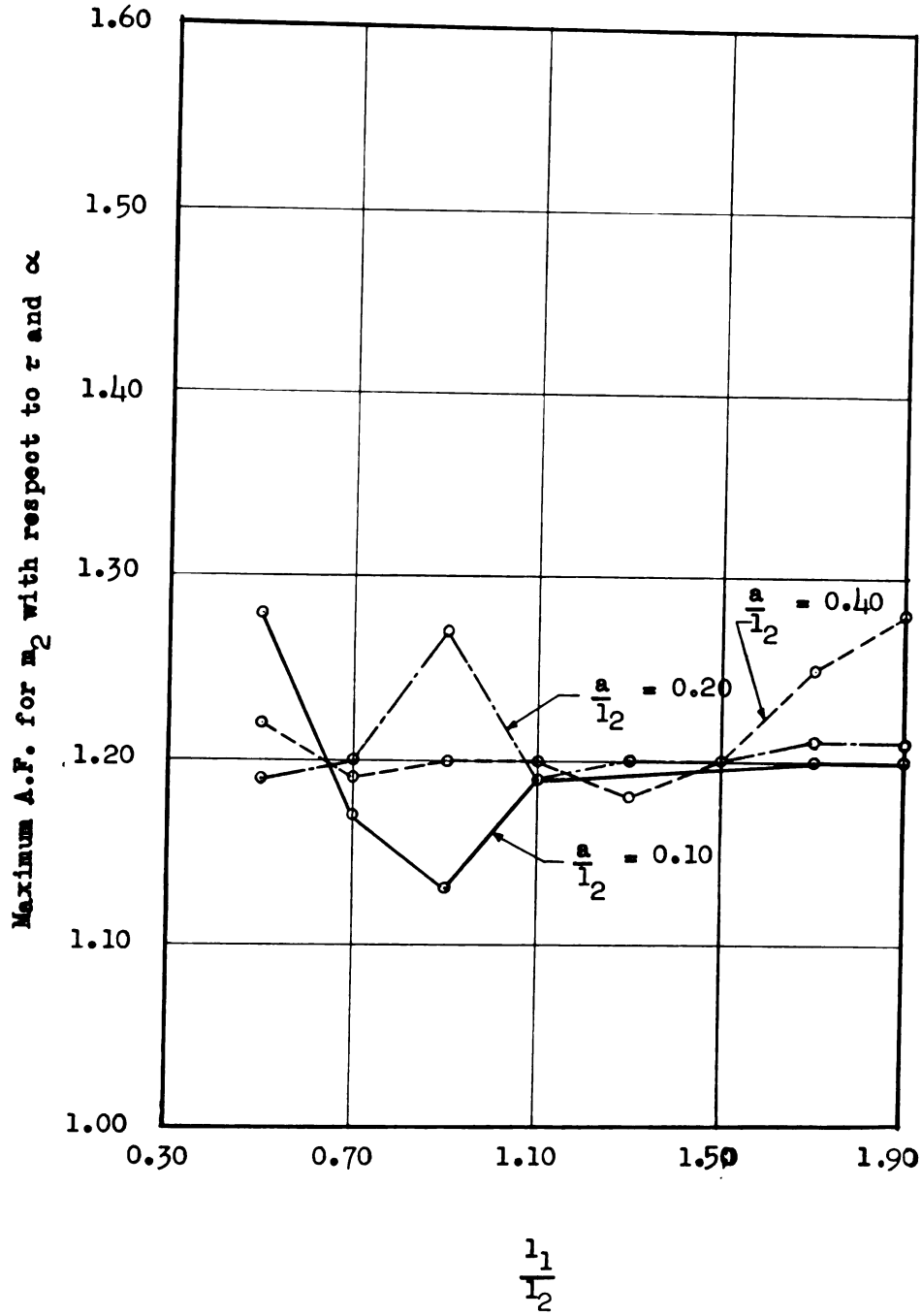

Fig. 20 - Maximum amplification factor for m_2

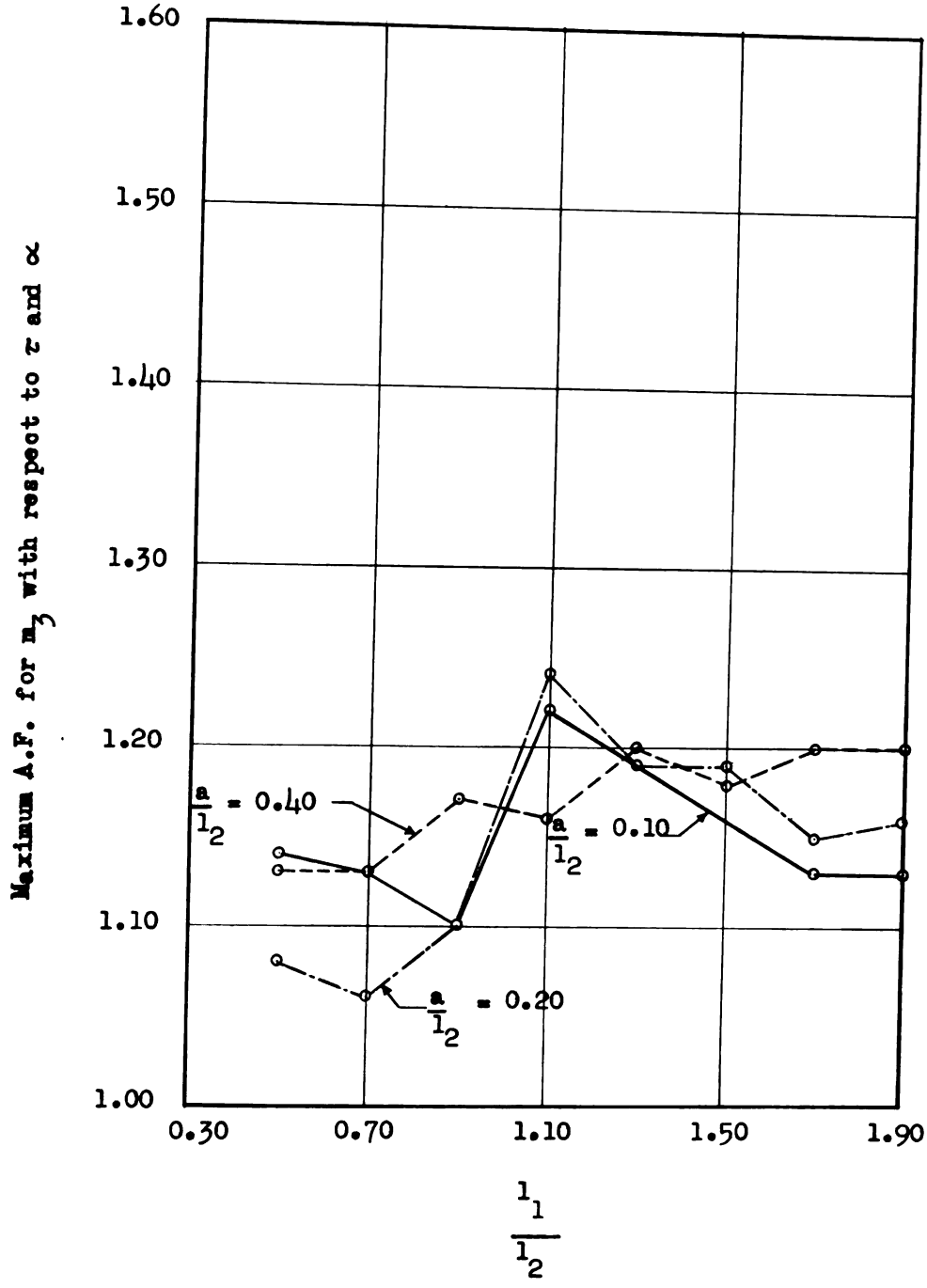

Fig. 21 - Maximum amplification factor for m_3

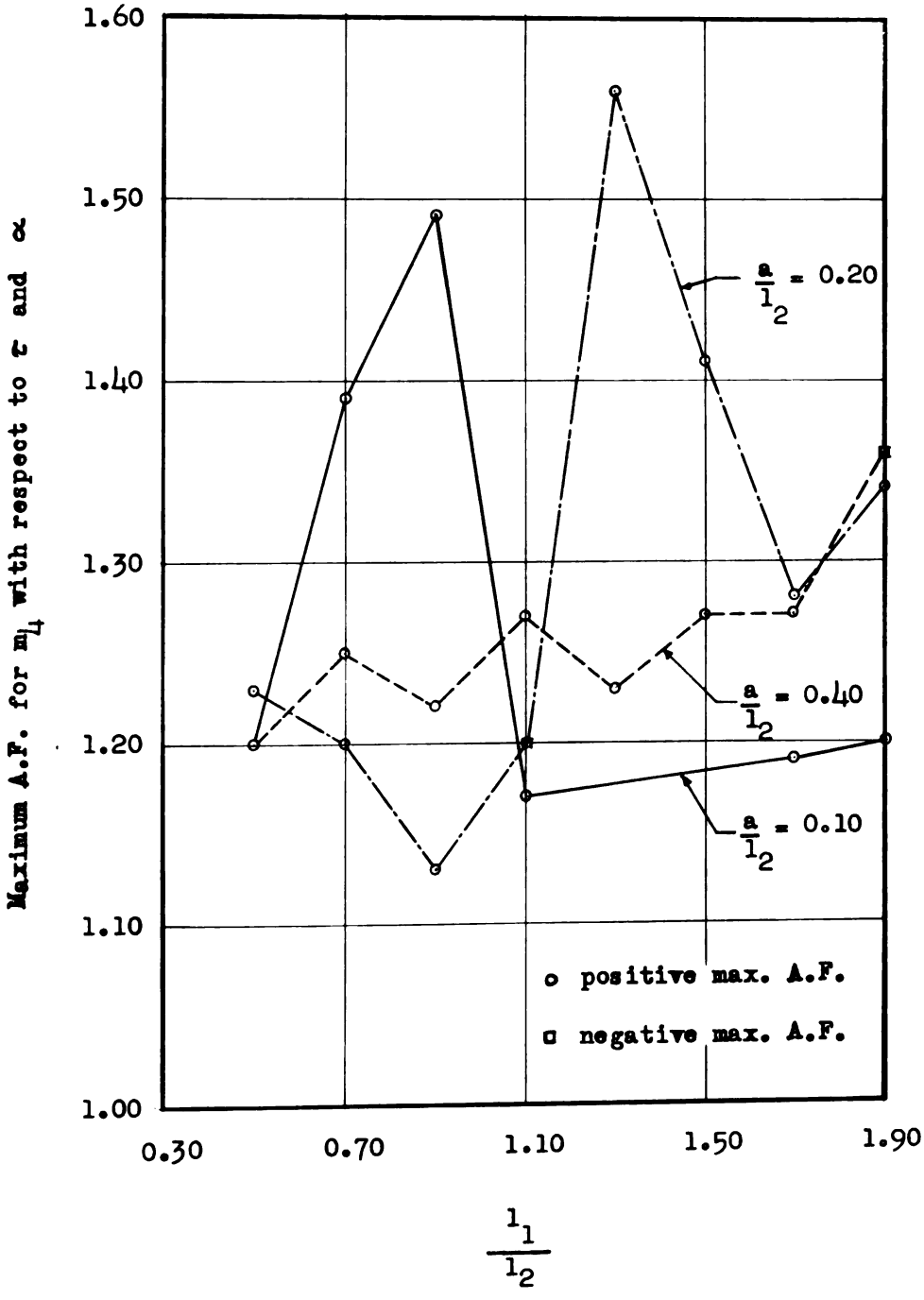

Fig. 22 - Maximum amplification factor for m_4

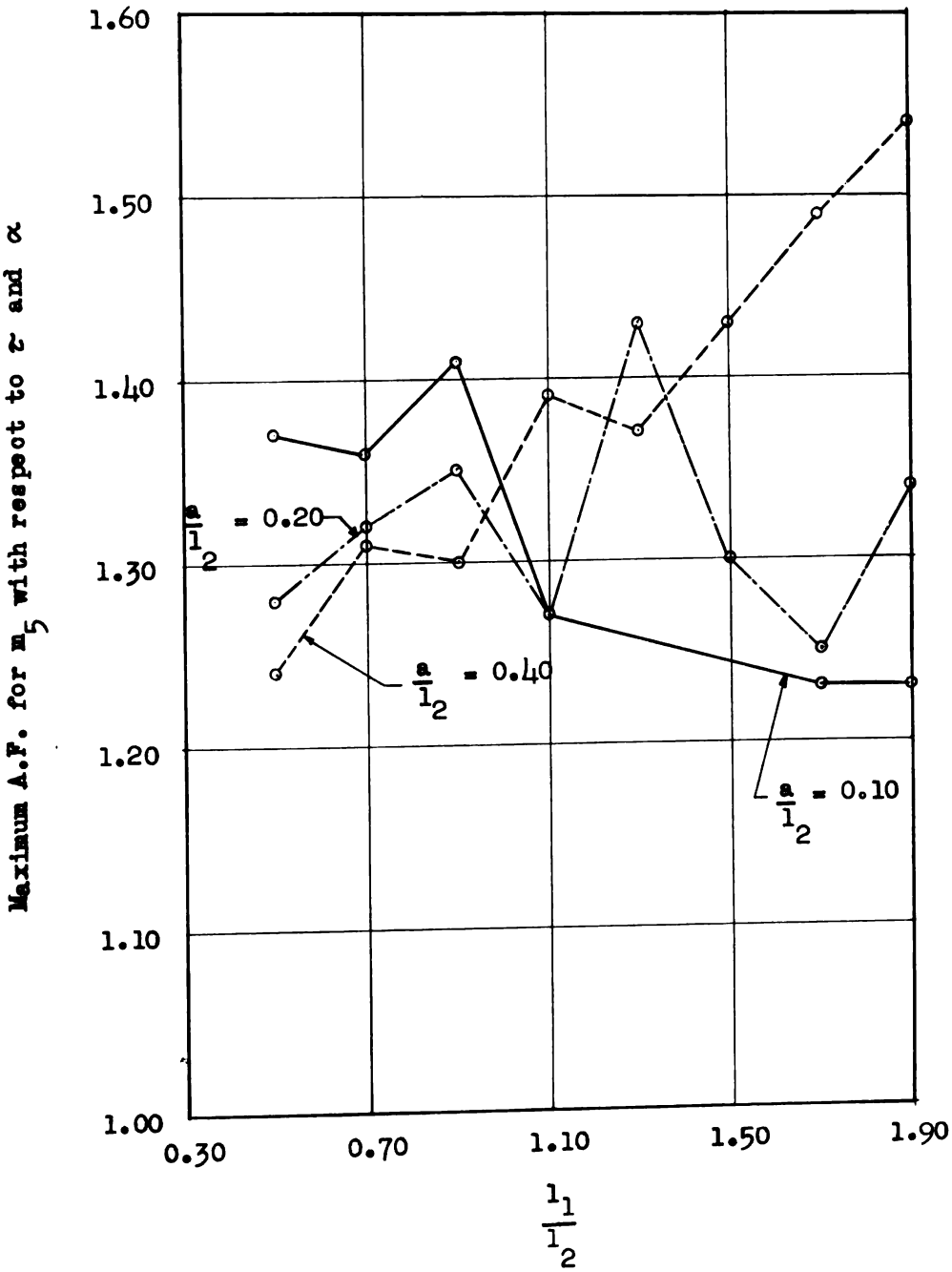

Fig. 23 - Maximum amplification factor for m_5